Electronic Supplementary Material (ESI) for Dalton Transactions.

S1. Experimental section **S2**

S1.1. General information **S2**

S1.2. Synthetic procedures **S4**

S1.3. NMR spectra **S8**

S1.4. Mass spectrometry data **S11**

S1.5. Chiral HPLC separations **S14**

S1.6. X-ray crystallographic data **S18**

S1.7. Photophysical and chiroptical measurements **S19**

S2. Computational section **S23**

S2.1. Computational details **S23**

S2.2. Additional calculated data **S24**

S2.3. Cartesian coordinates for optimized structures **S49**

S3. References **S57**

S1. Experimental section

S1.1. General information

Materials and methods: Experiments were performed using standard Schlenk techniques. Column chromatography purifications were performed in air over silica gel (Macherey Nagel 60 M, 0.04–0.063 mm). Irradiation reactions were conducted using a Heraeus TQ 150 mercury vapor lamp. All reactions were monitored by TLC analysis and visualizations were accomplished by irradiation with a UV light at 254 nm and 356 nm. THF was dried using Na/Benzophenone method. Dry DMSO over molecular sieves and dried acetonitrile were purchased from Sigma-Aldrich and were directly used without any further treatment. Dry toluene was obtained from an MB-SPS-800 distillation machine and was degassed by an argon bubbling for at least 30 minutes before use. Other reagents or solvents were purchased from Sigma-Aldrich, Alfa Aesar, ABCR and Fluorochem, and were used as received unless otherwise noted. Sodium carbonate was dried in a 110 °C oven for several days and stored at the same temperature.

NMR spectroscopy: ^{1}H and $^{13}C\{^{1}H\}$ NMR spectra were recorded at room temperature on a Bruker Avance III 400 MHz spectrometer equipped with a tunable BBFO probe. Chemical shifts δ are given in ppm, and coupling constants J in Hz. ^{1}H and ^{13}C NMR chemical shifts were determined using residual signals of the deuterated solvents, either deuterated dichloromethane (^{1}H δ = 5.32 ppm, ^{13}C δ = 54.0 ppm) or deuterated chloroform (^{1}H δ = 7.26 ppm, ^{13}C δ = 77.2 ppm). The terms s, d, t, m indicate respectively singlet, doublet, triplet, multiplet, while dd stands for doublet of doublets. Assignments of proton and carbon signals are based on COSY, edited-HSQC, and HMBC experiments.

Chiral high-performance liquid chromatography (HPLC): HPLC was performed at iSm2, Aix Marseille University, in an Agilent Technologies 1260 Infinity with Igloo-Cil ovens, using Jasco OR-1590 and CD-2095 as polarimetric and circular dichroism detectors. The analytical (250 x 4.6 mm) and preparative (250 x 10 mm) columns used were Chiralpak IA for complex **Pt1** and Chiralpak IF for **Pt2**.

High-resolution mass spectrometry (HR-MS): HRMS measurements were performed at the CRMPO, University of Rennes 1.

Polarimetry: Optical rotations were measured on a Jasco P-2000 polarimeter with a sodium lamp (589 nm) in a 1 cm cell, thermally equilibrated at 25 °C with a Peltier controlled cell holder. Specific rotation parameters are given in $deg \cdot mL \cdot g^{-1} \cdot dm^{-1}$.

UV-vis spectroscopy and electronic circular dichroism (ECD): UV-vis spectroscopy measurements were conducted on a Jasco-V630 spectrometer. Electronic circular dichroism (in $M^{-1} \cdot cm^{-1}$) was measured on a Jasco J-815 Circular Dichroism Spectrometer IFR140 facility, using the PRISM core (Biogenouest©, UMS Biosit, Université de Rennes 1 - Campus de Villejean-35043 Rennes Cedex, France).

Luminescence spectroscopy: Samples for emission measurements in toluene were contained within quartz cuvettes of 1 cm path length modified to allow connection to a high-vacuum line. Degassing was achieved via a minimum of three freeze-pump-thaw cycles whilst connected to the vacuum manifold; final vapour pressure at 77 K was < 5×10^{-2} mbar, as monitored using a Pirani gauge. Spectra were recorded on a Jobin Yvon Fluoromax-2 spectrofluorimeter with an R928 PMT detector and corrected for the wavelength dependence of the monochromator and detector. Luminescence quantum yields were determined using $[Ru(bpy)_3]Cl_2$ in aqueous solution as the standard (ϕ = 0.040).[1] The estimated uncertainty in the quoted lifetimes is ±20% of the value or better. Luminescence lifetimes of the

complexes were measured following excitation of the samples using a microsecond pulsed xenon flashlamp. The emitted light was detected at 90° to the excitation source using a Peltier-cooled R928 PMT, thermoelectrically-cooled to –20 °C and operating in multichannel scaling mode, after passage through a monochromator. The decays were much longer than the instrument response and were analyzed by least-squares tail-fitting to the following equation:

$I(t) = I(0)\cdot\exp(-kt) + c$

where $I(t)$ is the intensity of light detected at time t, k is the first-order rate constant for decay ($k = 1 / t$), and c is a constant reflecting the intrinsic "dark count" during the measurement. The quality of the fit was assessed by referring to the residuals (difference between fit and experimental data). The estimated uncertainty in the quoted lifetimes is ±10% or better.

Emission spectra and quantum yields of thin films were recorded using a Jobin Yvon Quanta-ϕ integrating sphere, operated in conjunction with a Fluorolog spectrometer through the usual of optical fibres. The samples were prepared from toluene solutions of 2 wt% of the Pt(II) complex in PMMA (molecular weight approx. 35000), and dried following drop-casting upon quartz substrates. The sample chamber was purged with nitrogen gas for at least 10 minutes prior to data acquisition; the displacement of oxygen can be readily monitored from the increase and subsequent plateauing of the emission intensity at λ_{max}. A similar approach was used to measure the lifetimes of the films under inert conditions, the decays being analyzed as described above.

Circularly polarized luminescence: Circularly polarized luminescence (CPL) measurements were performed using a home-built CPL spectrofluoropolarimeter (constructed with the help of the JASCO Company). The samples were excited using a 90° geometry with a xenon ozone-free lamp 150 W LS. The concentration of the samples was ca. 10^{-5} M.

CPL measurements on films: Circular polarization of luminescence from films was measured using a home-built spectrometer, involving photoelastic modulator (PEM) at 50 kHz, parallel multichannel detection and single photon counting electronics (see Scheme S1.1). In the polarization measurement, the emission collection and photoexcitation were performed in a direction perpendicular to the luminescent layer and with an in-line geometry. Excitation light was depolarized by sending it through an optical fiber. Photon counting detection is used. An electronic gate is used to reject incoming photocurrent pulses during the time intervals in the modulation cycle of the PEM where the modulation depth is not sufficiently deep. This so-called modulation window was set to 50% of the total cycle. Photocurrent pulses that pass the gate are then counted as left circularly polarized (N_L) or right circularly polarized (N_R) photons. After completing the measurement, the degree of circular polarization is obtained from the total number of L and R photons counted using $g_{lum} = 2(N_L-N_R)/(N_L+N_R)$. The g_{lum} values reported are the average of about 60 consecutive measurements lasting each one minute. The error bars represent the standard error of the average g_{lum}.

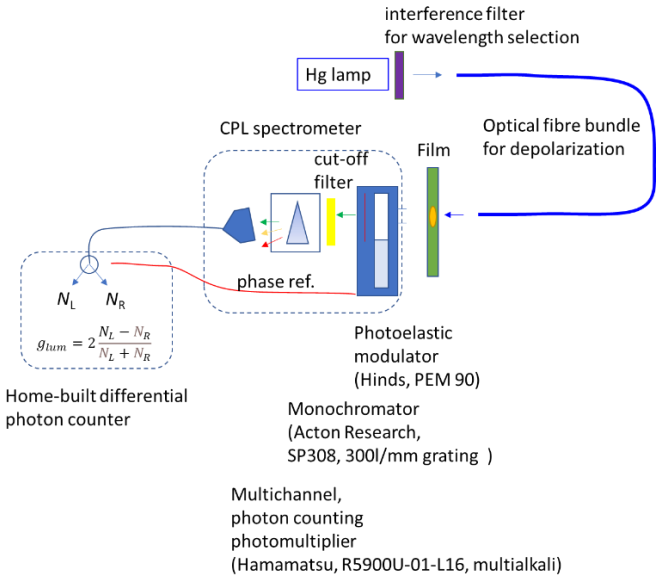

Scheme S1.1: *Schematic representation of experimental setup for CPL measurement of film.*

S1.2. Synthetic procedures

3*H*-benzo[5,6]phenanthro[3,4-*d*]imidazole **1** was prepared according to the literature.[2] Compounds **2** and **3** were prepared following procedures similar to those previously developed in our group.[3] Synthetic pathway to helicene-NHC-platinum(II) complexes studied in this work is shown in Scheme S1.2.

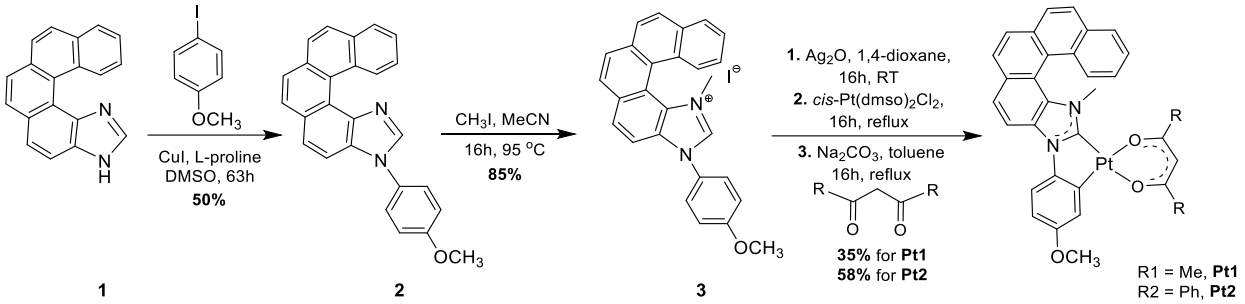

Scheme S1.2: *General synthetic route to prepare helicene-NHC-platinum(II) complexes studied in this work.*

3-(4-methoxy-phenyl)-3*H*-benzo[5,6]phenanthro[3,4-*d*]imidazole (2)

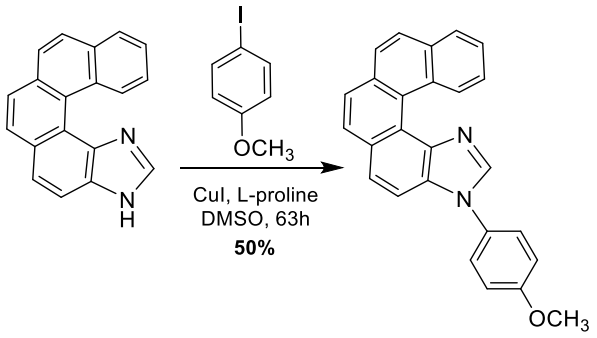

1 **2**

In a flame-dried Schlenk flask equipped with a rubber septum and under argon, **1** (95 mg, 0.35 mmol), 4-iodoanisole (134 mg, 0.44 mmol), dried K_2CO_3 (145 mg, 1.40 mmol), CuI (7 mg, 0.04 mmol) and L-proline (8 mg, 0.07 mmol) were dissolved in anhydrous dimethylsulfoxyde (DMSO, 3 mL). The rubber septum was replaced by a Teflon cap, and the medium was degassed with a freeze/pump/thaw procedure applied three times to ensure an air- and oxygen-free atmosphere. The reaction mixture was then heated at 110 °C for 63 h. The mixture was allowed to cool down to room temperature, and the medium was diluted with distilled water and CH_2Cl_2. The aqueous layer was then extracted using CH_2Cl_2 three times, and the combined organic layers were washed with water twice. The organic phase was dried over $MgSO_4$, filtered, and the solvent was evaporated under reduced pressure. The obtained crude was then purified by column chromatography (SiO_2, *n*-heptane / EtOAc = 8:2 to 1:1) to afford 3-(4-methoxy-phenyl)-3*H*-benzo[5,6]phenanthro[3,4-*d*]imidazole **2** as a white solid (78 mg , 50% yield).

^{1}H NMR (400 MHz, CD_2Cl_2, δ ppm): δ = 3.91 (s, 3H, O-CH_3), 7.14 (d, *J* = 8.9 Hz, 2H, CH_{Ph}), 7.53 (m, *J* = 8.6 Hz, 3H, CH_{Ar} + CH_{Ph}), 7.61 (t, *J* = 7.7 Hz 1H, CH_{Ar}), 7.76 (d, *J* = 8.9 Hz 1H, CH_{Ar}), 7.84 (d, *J* = 8.4 Hz, 1H, CH_{Ar}), 7.88 (d, *J* = 8.5 Hz, 1H, CH_{Ar}), 7.91 - 8.05 (m, 4H, CH_{Arl}), 8.09 (s, 1H,N-C*H*-N), 9.16 (d, *J* = 8.6 Hz, 1H, CH_{Ar}).

^{13}C{^{1}H} NMR (101 MHz, $CDCl_3$, δ ppm): δ = 56.1 (O-*C*H$_3$), 111.4 (*C*$_{Ar}$), 115.5 (*C*$_{Ph}$), 115.5 (*C*$_{Ph}$), 123.7(*C*$_{Ar}$), 124.2(*C*$_{Ar}$), 125.4(*C*$_{Ar}$), 125.5(*C*$_{Ar}$), 126.5(*C*$_{Ar}$), 126.6 (*C*$_{Ph}$), 126.6 (*C*$_{Ph}$), 126.8(*C*$_{Ar}$), 127.2(*C*$_{Ar}$), 128.3(*C*$_{Ar}$), 128.3(*C*$_{Ar}$), 128.4(*C*$_{Ar}$), 129.5(*C*$_{Ar}$), 130.8(*C*$_{Ar}$), 131.2(*C*$_{Ar}$), 131.4(*C*$_{Ar}$), 132.6(*C*$_{Ar}$), 132.9(*C*$_{Ar}$), 133.3(*C*$_{Ar}$), 139.3(*C*$_{Ar}$), 140.7(N-*C*$_{Ph}$), 160.0 (s, N-*C*-N).

HRMS (ESI): m/z calculated for [$C_{26}H_{19}N_2O$] ($M+H^+$): 375.1492; found, 375.1492.

1-methyl-3-(4-methoxy-phenyl)-3*H*-benzo[5,6]phenanthro[3,4-*d*]imidazole-1-ium iodide salt (3)

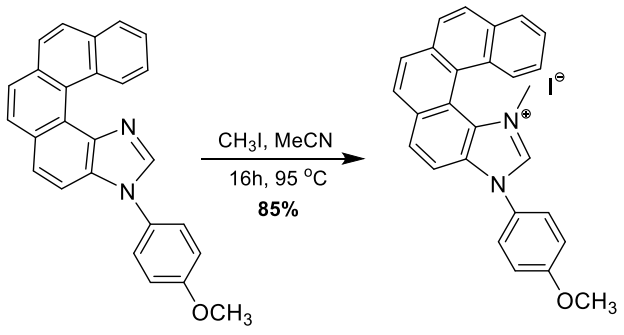

2 **3**

In a flame-dried Schlenk flask, **2** (80 mg, 0.22 mmol) was places and, after two vacuum/argon cycles, dried acetonitrile (8 mL) was added. Under argon, an excess of methyl iodide (0.15 mL, 2.40 mmol) was added. The reaction mixture was then sealed with a Teflon cap and heated at 95 °C overnight. The resulting heterogeneous mixture was finally allowed to cool down to room temperature, and the solvent was evaporated under vacuum. The obtained solid was washed and triturated three times with ethyl acetate and diethyl ether to afford pure 1-methyl-3-(4-methoxy-phenyl)-3*H*-benzo[5,6]phenanthro[3,4-*d*]imidazole-1-ium iodide salt **3** as a white-off solid (93 mg, 85% yield).

^{1}H NMR (400 MHz, CD_2Cl_2, δ ppm): δ = 3.63 (s, 3H, N-CH_3), 3.96 (s, 3H, O-CH_3), 7.31 – 7.21 (m, 2H, CH_{Ar}), 7.69 (dd, *J* = 7.0, 1.6 Hz, 2H, CH_{Ph}), 7.85 (d, *J* = 8.9 Hz, 1H, CH_{Ar}), 7.96 – 8.05 (m, 3H CH_{Ar} & C-H_{Ph}), 8.06 – 8.17 (m, 4H, CH_{Ar}), 8.20 (d, *J* = 8.9 Hz, 1H, CH_{Ar}), 8.36 (dd, *J* = 7.6, 1.7 Hz, 1H, CH_{Ar}), 10.70 (s, 1H, N-C*H*-N).

^{13}C {^{1}H} NMR: was not resolved enough due to poor solubility of the compound.

HRMS (ESI): m/z calculated for $[C_{27}H_{21}N_2O]^+$: 389.1648; found, 389.1646.

[5]helicene-NHC cyclometalated platinum(II) complexes (Pt1, Pt2)

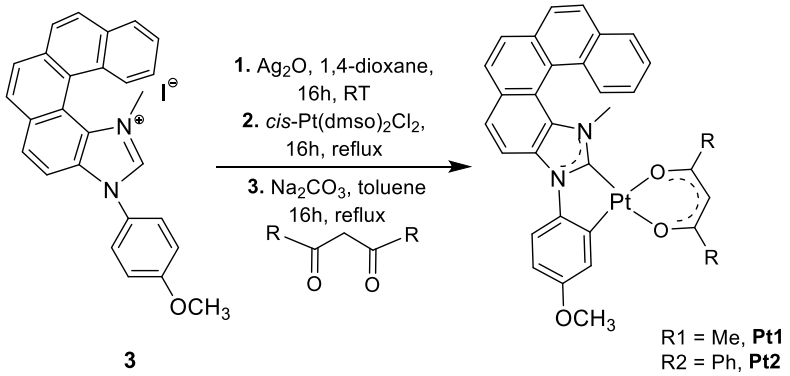

3

In a flame-dried Schlenk flask equipped with a rubber septum, imidazolium salt **3** (90 mg, 0.17 mmol) and silver(I) oxide (24 mg, 0.11 mmol) were dissolved in 10 mL of 1,4-dioxane and stirred for 16 h at room temperature under argon atmosphere. Freshly prepared *cis*-platinum(II)-bis-dimethylsulfoxide-dichloride (88 mg, 0.18 mmol) was added to the mixture, which was subsequently heated to reflux (110 °C) for 16 h. The solvent was then removed, and the residue was dissolved in 10 mL of toluene. 2,4-pentanedione (100 mg, 1 mmol) or 1,3-diphenyl-1,3-propanedione (224 mg, 1 mmol) and dried sodium carbonate (106 mg, 1.00 mmol) were added, and the reaction mixture was stirred for 16 h at 110 °C. The solvent was then removed, and the residue was washed with water, followed by column chromatography (heptane / ethyl acetate = 90:10) to afford pure platinum complexes as yellow solids, **Pt1** (41 mg, 35% yield) and **Pt2** (80 mg, 58% yield).

Compound Pt1:

^{1}H NMR (400 MHz, CD_2Cl_2, δ ppm): δ = 1.85 (s, 3H, CH_3), 2.08 (s, 3H, CH_3), 3.37 (s, 3H, N-CH_3), 3.88 (s, 3H, OCH_3), 5.53 (s, 1H, CH_{acac}), 6.75 (dd, *J* = 8.7, 2.9 Hz, 1H, CH_{Ph}), 7.46 (d, *J* = 2.8 Hz, 1H, CH_{Ph}), 7.55 (m, 1H, CH_{Ar}), 7.62 (m, 2H, CH_{Ph} & CH_{Ar}), 7.88 – 8.08 (m, 6H, CH_{Ar}), 8.32 (d, *J* = 8.7 Hz, 1H, CH_{Ar}), 8.34 (d, *J* = 8.4 Hz, 1H, CH_{Ar}).

$^{13}C\{^1H\}$ NMR (75 MHz, CD_2Cl_2, δ ppm): δ = 27.9 (*C*H_3), 28.0 (*C*H_3), 37.5 (N-*C*H_3), 55.7 (O-*C*H_3), 102.1 (*C*H_{acac}), 108.1 (*C*H_{Ph}), 111.0 (*C*H_{Ar}), 112.8 (*C*H_{Ph}), 116.5 (C_{Ar}), 117.6 (*C*H_{Ph}), 124.5 (C_{Ar}), 125.4 (*C*H_{Ar}), 126.0 (*C*H_{Ar}), 126.1 (*C*H_{Ar}), 126.3 (*C*H_{Ar}), 126.8 (*C*H_{Ar}), 126.8 (*C*H_{Ar}), 128.0 (*C*H_{Ar}), 128.6 (*C*H_{Ar}), 128.7 (*C*H_{Ar}), 128.9 (C_{Ar}), 131.0 (C_{Ar}), 131.1 (C_{Ar}), 131.7 (C_{Ar}), 132.2 (C_{Ar}), 132.5 (C_{Ar}), 133.4 (C_{Ar}), 142.3 (C_{Ar}-Pt), 156.2 (C_{Ar}-O), 160.3 ($C_{carbene}$-Pt), 185.4 (*C*=O), 186.1 (*C*=O).

HRMS : m/z calculated for $[C_{32}H_{26}N_2O_3{}^{195}Pt]^+$: 681.1586; found, 681.1590.

Compound Pt2:

^1H NMR (400 MHz, CD_2Cl_2, δ ppm): δ = 3.44 (s, 3H, N-C*H*$_3$), 3.93 (s, 3H, O-C*H*$_3$), 6.79 (dd, *J* = 8.1, 2.8 Hz, 1H, C*H*$_{Ph}$), 6.82 (s, 1H, C*H*$_{acac}$), 7.37 (t, *J* = 7.5 Hz, 2H, C*H*$_{Ph}$ & C*H*$_{Ar}$), 7.51 (t, *J* = 7.2 Hz, 3H, C*H*$_{dbm}$ & C*H*$_{Ar}$), 7.59 (m, 2H, C*H*$_{Ar}$), 7.64 (m, 2H, C*H*$_{Ph}$ & C*H*$_{Ar}$), 7.81 (d, *J* = 7.2 Hz, 2H, C*H*$_{dbm}$), 7.91 (d, *J* = 8.3 Hz, 1H, C*H*$_{Ar}$), 7.96 (d, *J* = 8.5 Hz, 1H, C*H*$_{Ar}$), 8.04 (m, 3H, C*H*$_{Ar}$), , 8.13 (m, 3H, C*H*$_{dbm}$ & C*H*$_{Ar}$), 8.34 (d, *J* = 8.3 Hz, 1H, C*H*$_{Ar}$), 8.42 (d, *J* = 8.3 Hz, 1H, C*H*$_{Ar}$).

$^{13}C\{^1H\}$ NMR (101 MHz, CD_2Cl_2, δ ppm): δ = 38.2 (N-*C*H_3), 55.7 (O-*C*H_3), 97.1(*C*H_{acac}), 109.0 (*C*H_{Ph}), 111.1 (*C*H_{Ar}), 113.0 (*C*H_{Ph}), 116.6 (C_{Ar}), 117.3 (*C*H_{Ar}), 124.5 (C_{Ar}), 125.5 (*C*H_{Ar}), 126.2 (*C*H_{Ar}), 126.2 (*C*H_{Ar}), 126.4 (*C*H_{Ar}), 126.6 (C_{Ar}), 126.7 (*C*H_{Ar}), 127.4 (*C*H_{dbm}), 127.4 (*C*H_{dbm}), 127.6 (*C*H_{dbm}), 127.6 (*C*H_{dbm}), 128.1 (C_{Ar}), 128.7 (*C*H_{Ar}), 128.8 (*C*H_{dbm}), 128.8 (C_{Ar}), 128.8 (*C*H_{dbm}), 128.8 (*C*H_{dbm}), 129.0 (*C*H_{dbm}), 129.0 (*C*H_{dbm}), 131.2 (*C*H_{Ar}), 131.2 (C_{Ar}), 131.4 (*C*H_{Ar}), 131.7 (C_{Ar}), 132.4 (C_{Ar}), 132.6 (C_{Ar}), 133.4 (C_{Ar}), 133.9 (C_{Ar}), 140.3 (C_{dbm}), 140.9 (C_{dbm}), 142.3 (C_{Ar}-Pt), 156.2 (C_{Ar}-O), 160.7 ($C_{carbene}$-Pt), 179.9(*C*=O), 181.0 (*C*=O).

HRMS (ESI): m/z calculated for $[C_{42}H_{30}N_2O_3{}^{195}Pt]^+$: 805.1899; found, 805.1900.

S1.3. NMR spectra

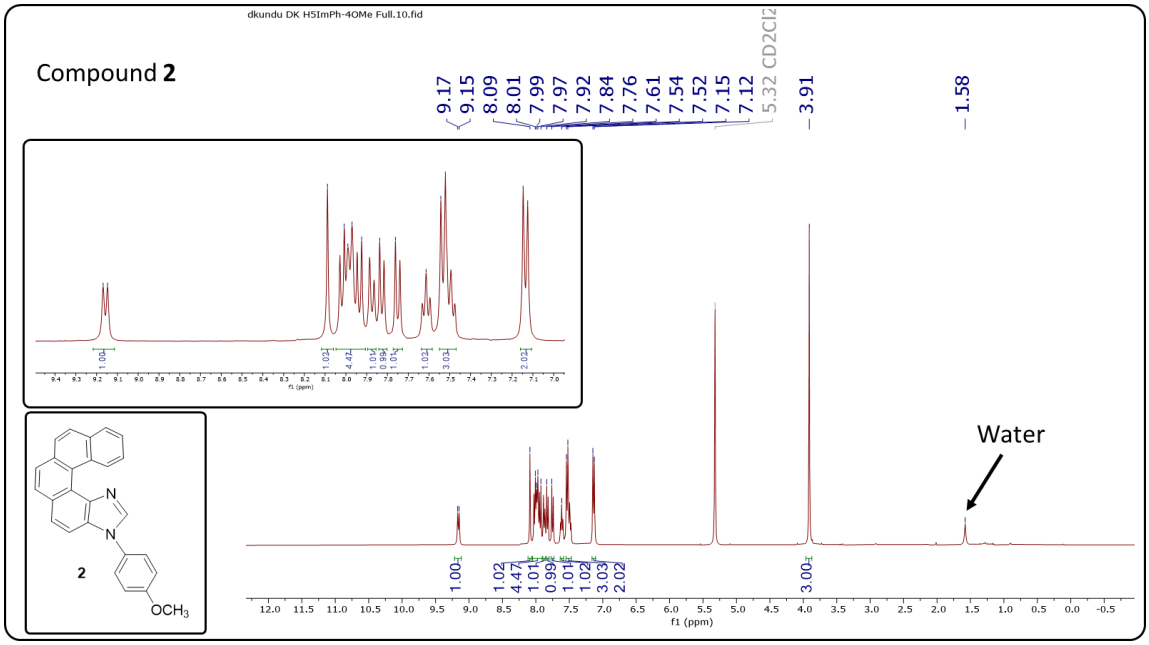

Figure S1.1: *^{1}H NMR spectrum of **2** in CD_2Cl_2 at 298 K (400 MHz).*

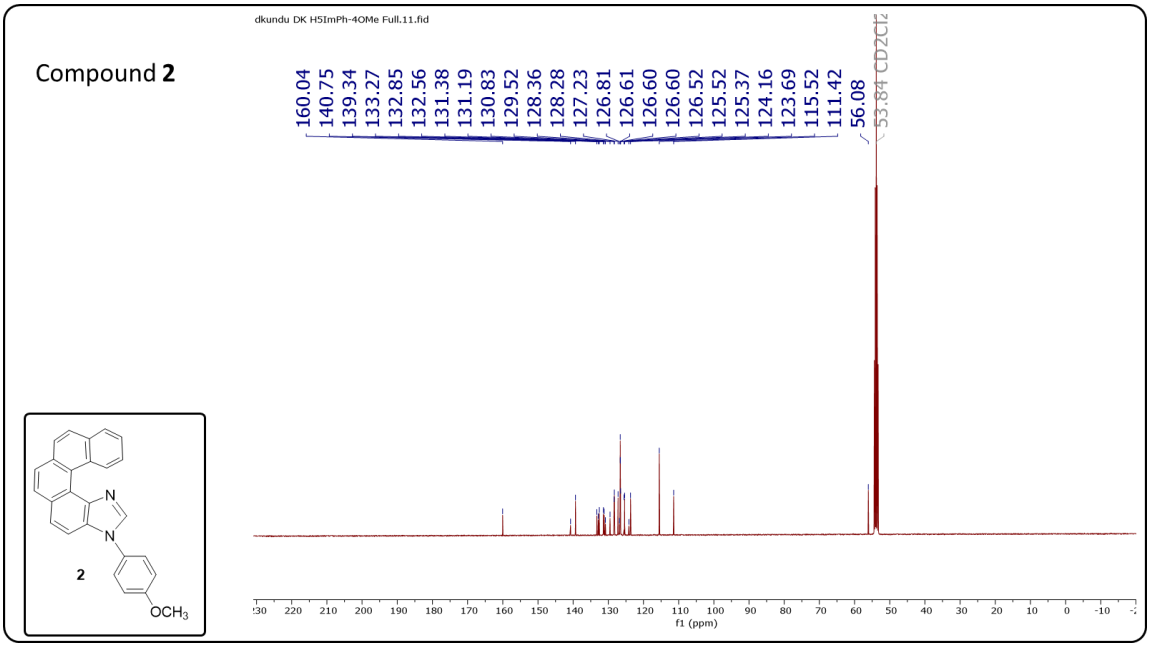

Figure S1.2: *$^{13}C\{^{1}H\}$ NMR spectrum of **2** in CD_2Cl_2 at 298 K (101 MHz).*

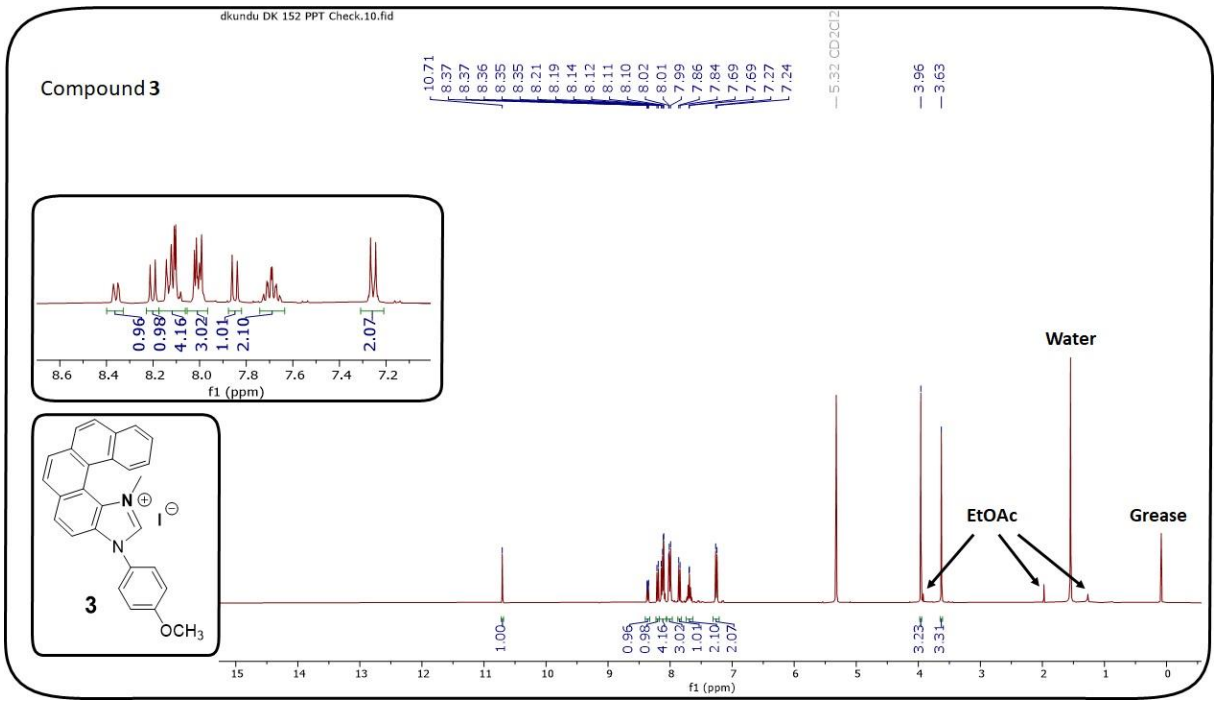

Figure S1.3: *^{1}H NMR spectrum of **3** in CD_2Cl_2 at 298 K (400 MHz).*

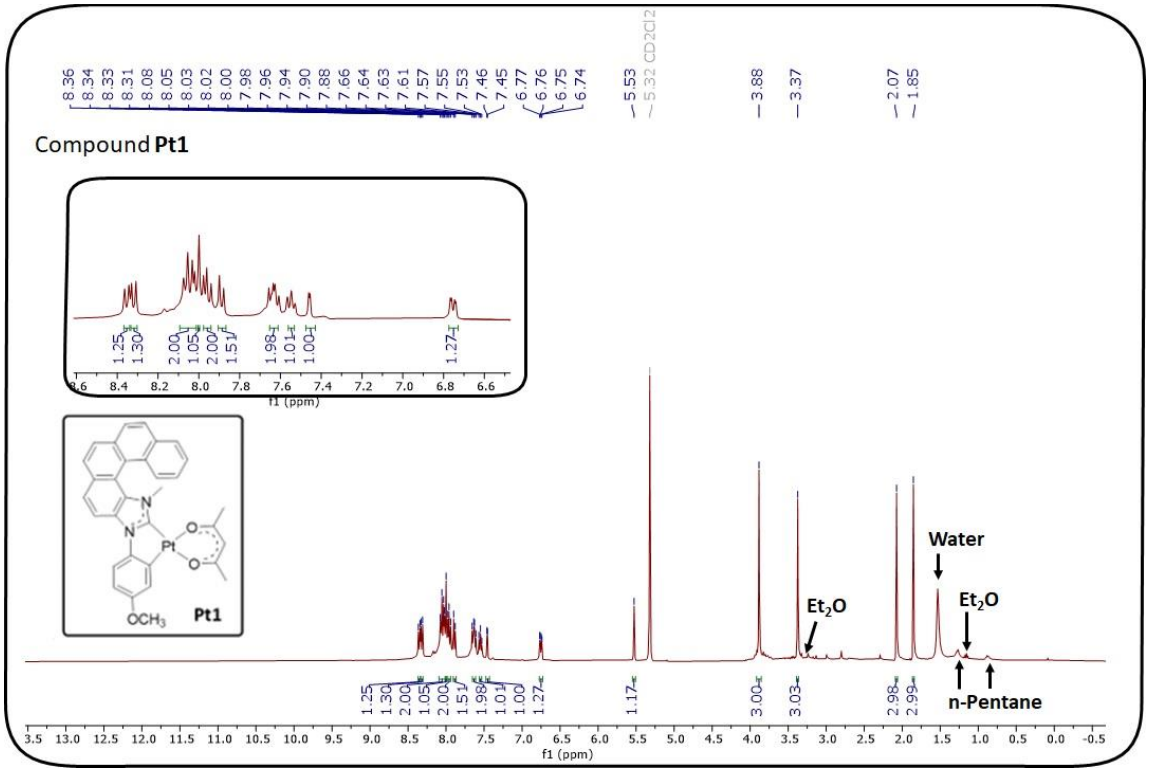

Figure S1.4: *^{1}H NMR spectrum of **Pt1** in CD_2Cl_2 at 298 K (400 MHz).* ***Note:*** *The compound is soluble enough in CD_2Cl_2 but show low stability and additional signals of lower intensity.*

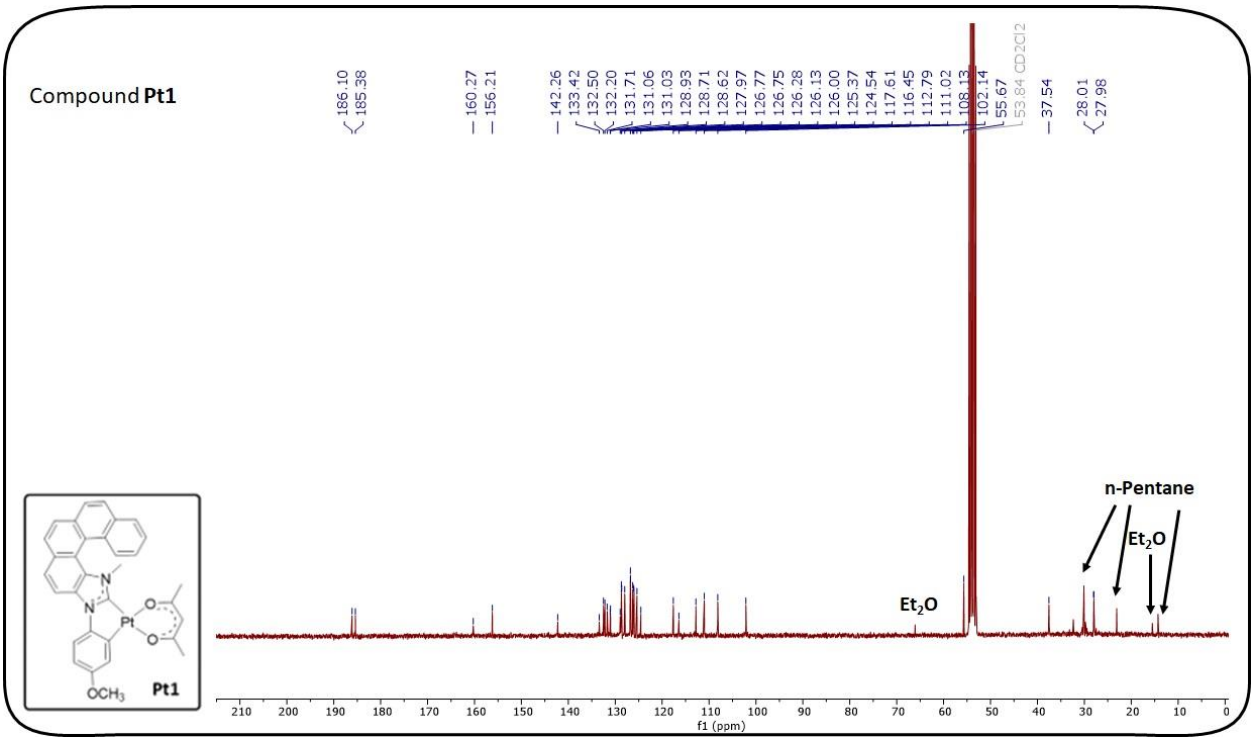

Figure S1.5: *$^{13}C\{^{1}H\}$ NMR spectrum of **Pt1** in CD_2Cl_2 at 298 K (75 MHz).* ***Note:*** *The compound is soluble enough in CD_2Cl_2 but show low stability and additional signals of lower intensity.*

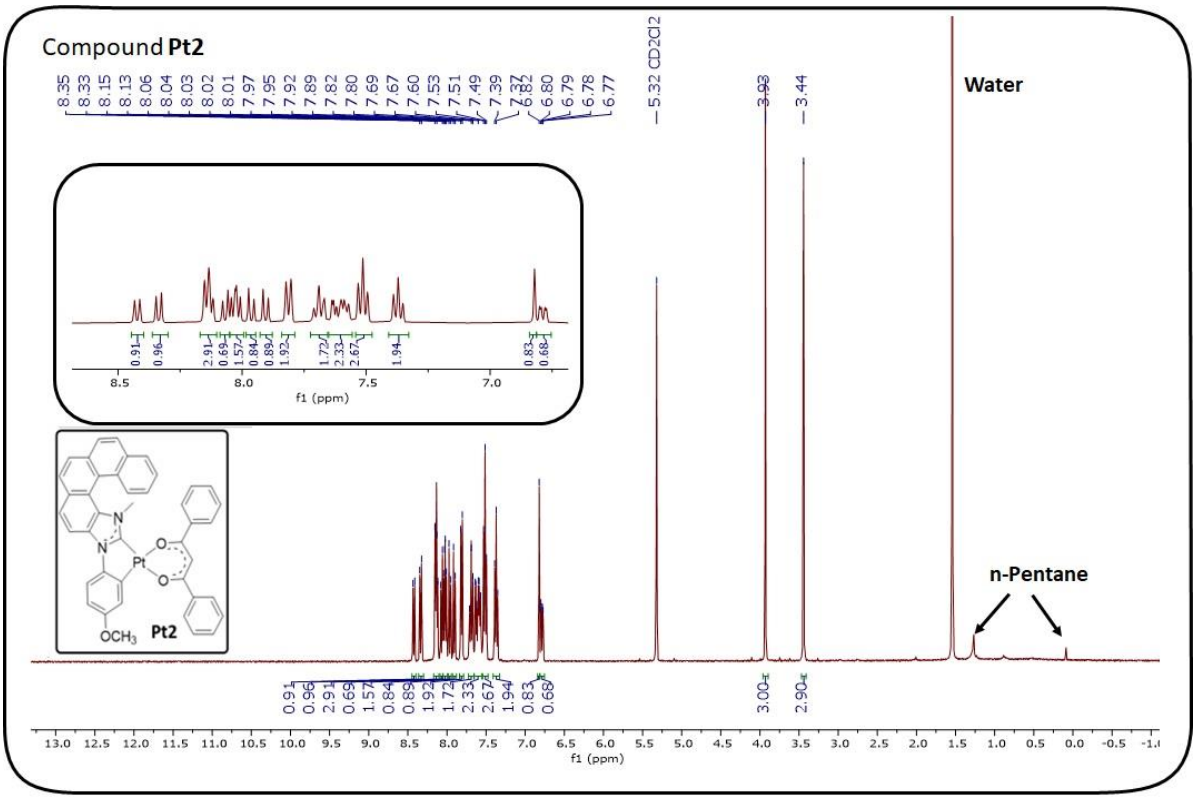

Figure S1.6: *^{1}H NMR spectrum of **Pt2** in CD_2Cl_2 at 298 K (400 MHz).*

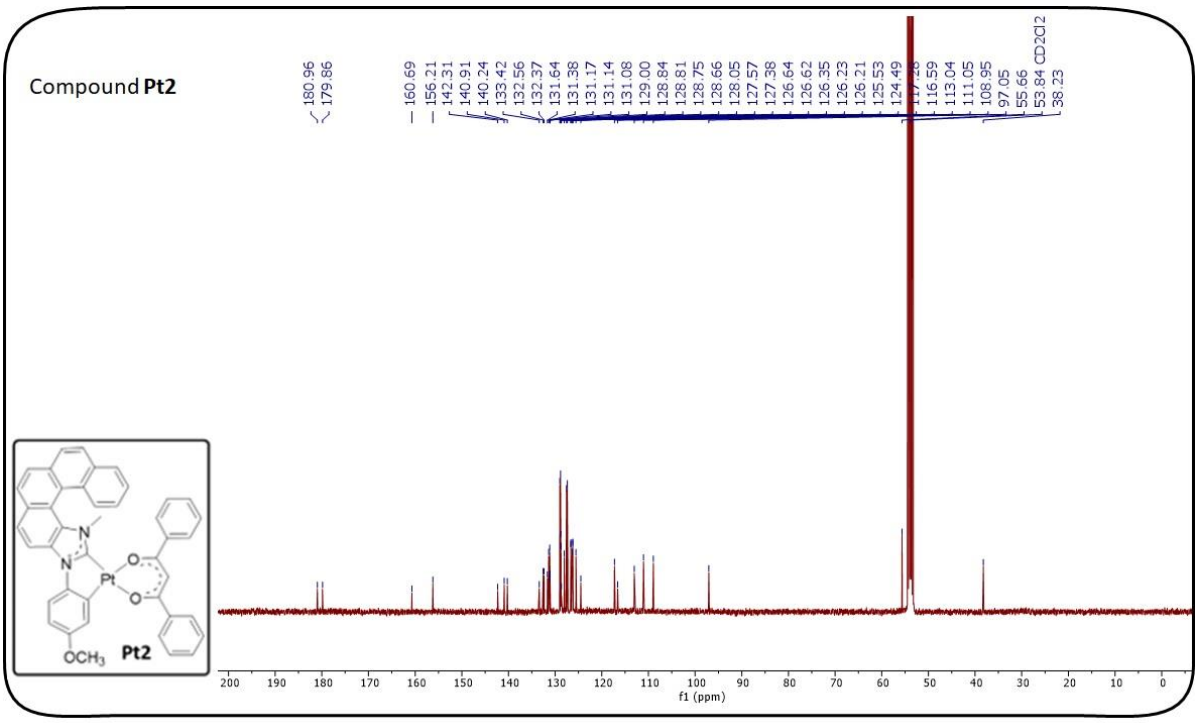

Figure S1.7: *$^{13}C\{^{1}H\}$ NMR spectrum of* ***Pt2*** *in CD_2Cl_2 at 298 K (101 MHz).*

S1.4. Mass spectrometry data

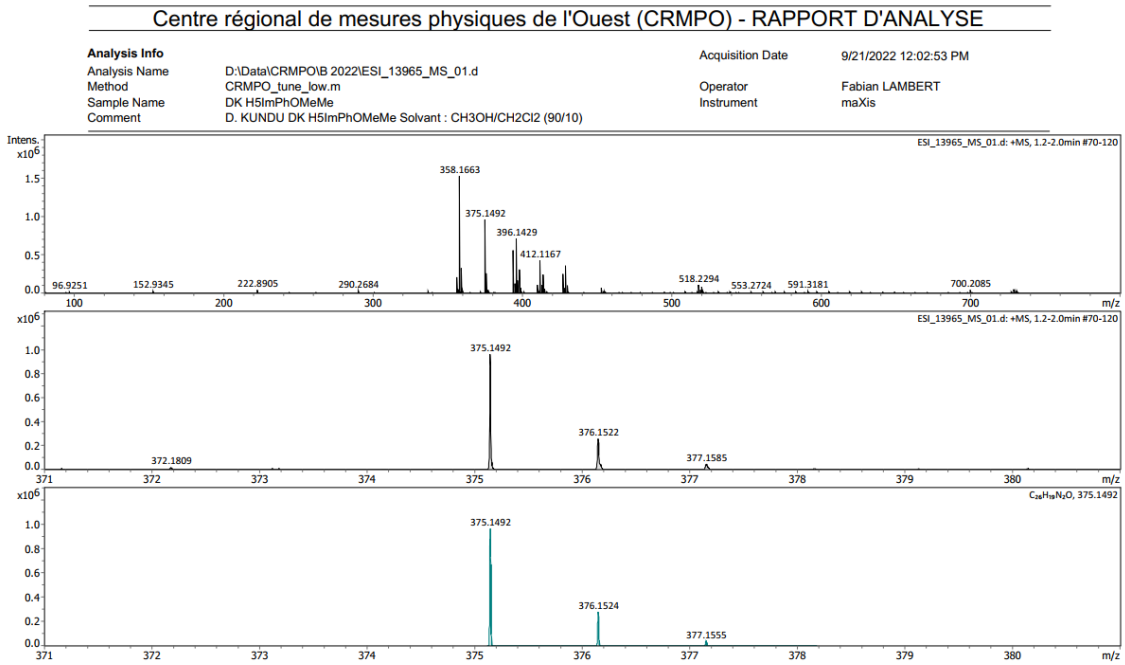

Figure S1.8: *High Resolution Mass Spectrometry analysis of* ***2****.*

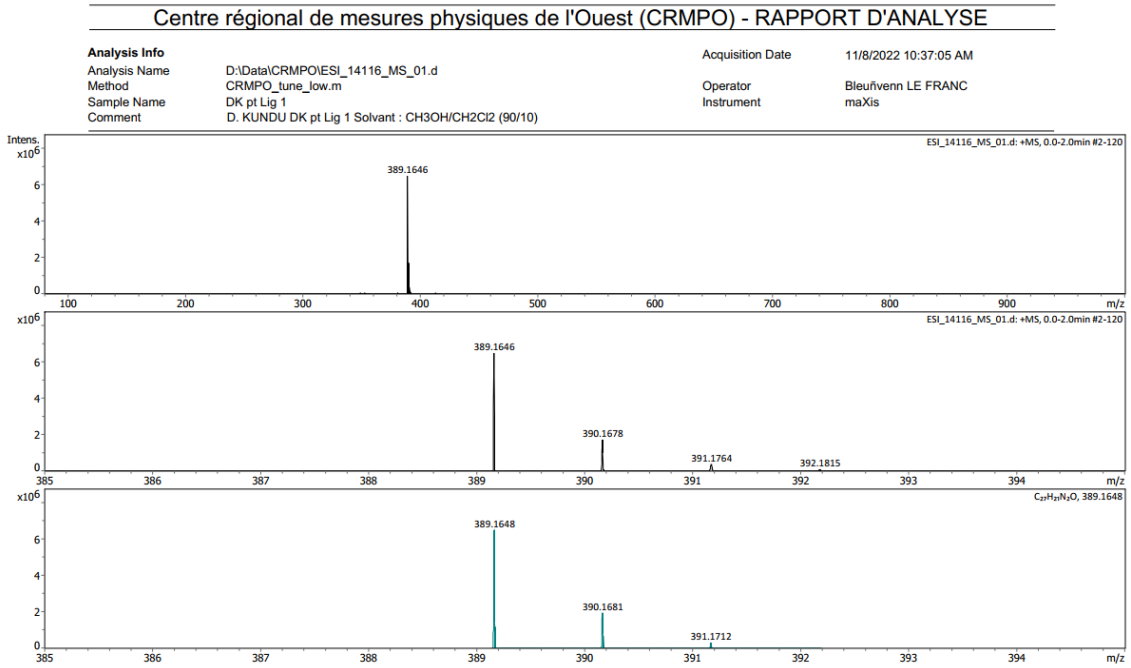

Figure S1.9: *High Resolution Mass Spectrometry analysis of* ***3****.*

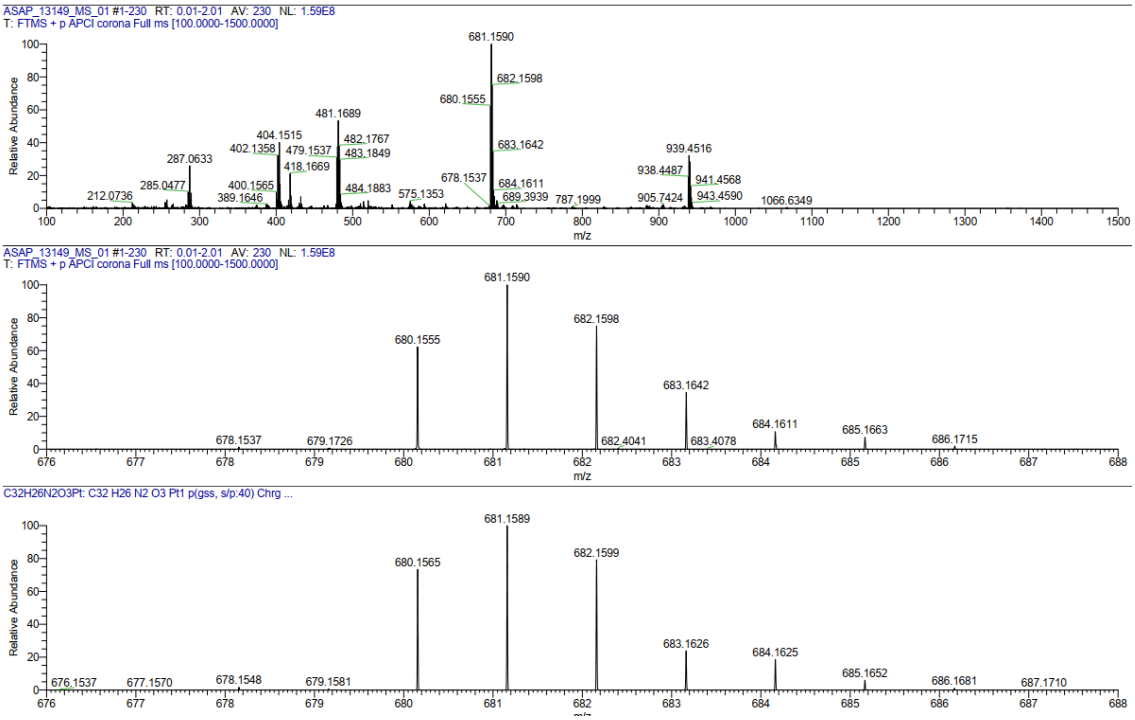

Figure S1.10: *High Resolution Mass Spectrometry analysis of* ***Pt1****.*

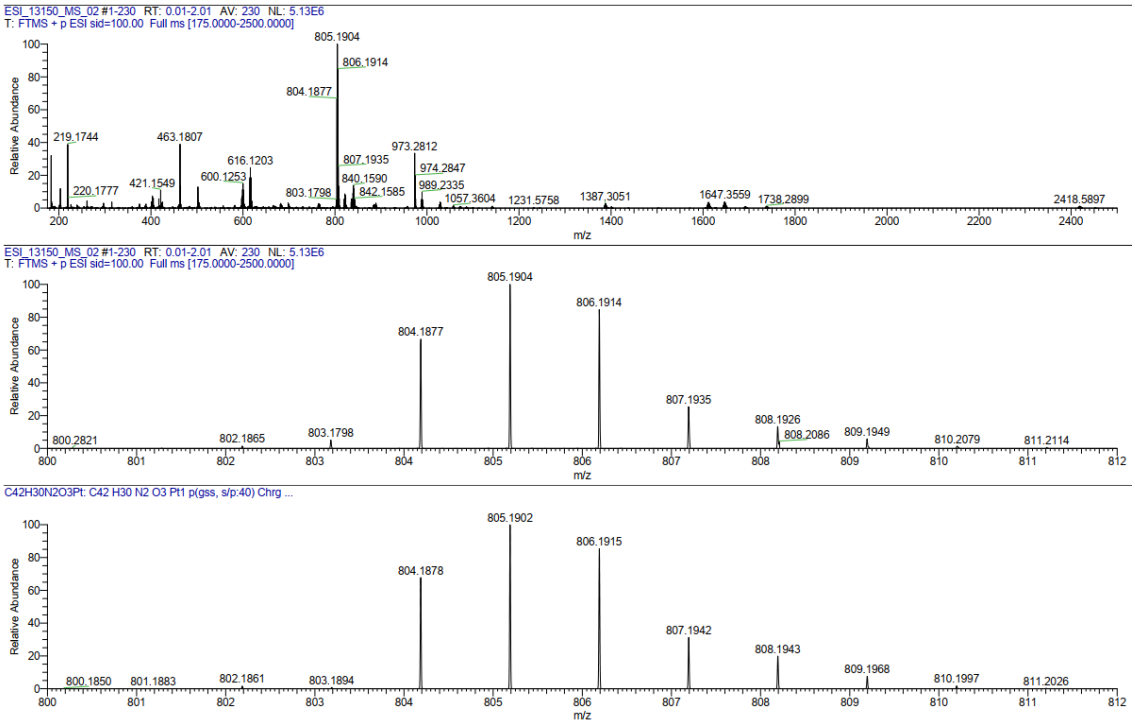

Figure S1.11: *High Resolution Mass Spectrometry analysis of* ***Pt2****.*

S1.5. Chiral HPLC separations

Analytical chiral HPLC separation for compound **Pt1**

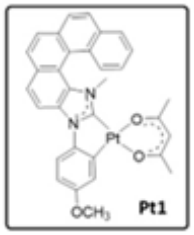

The sample is dissolved in dichloromethane, injected on the chiral column, and detected with a UV detector at 230 nm and a circular dichroism detector at 254 nm. The flow-rate is 1 mL/min.

Column	Mobile Phase	t1	k1	t2	k2	α	Rs
Chiralpak IA	heptane / 2-PrOH / dichloromethane (80/10/10)	5.92(+)	1.01	7.67 (-)	1.60	1.59	4.11

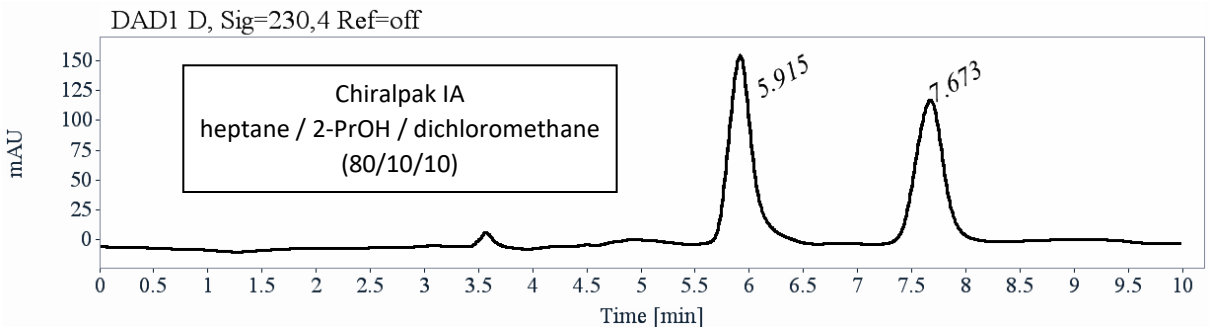

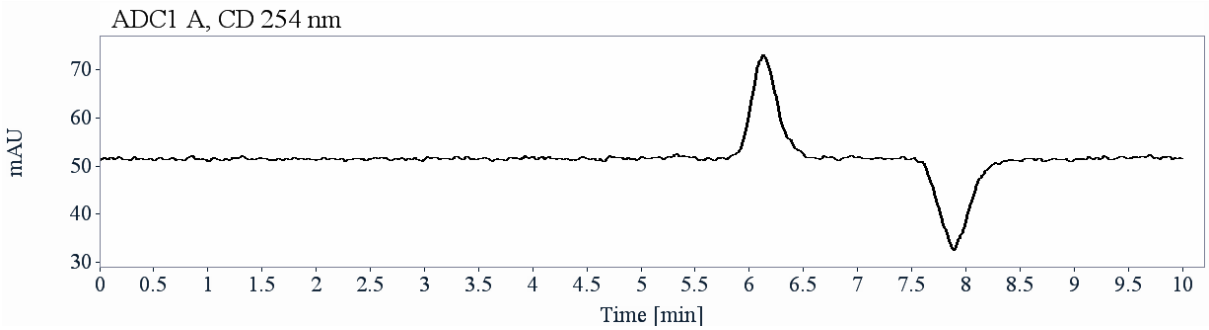

RT [min]	Area	Area%	Capacity Factor	Enantioselectivity	Resolution (USP)
5.92	2435	52.83	1.01		
7.67	2175	47.17	1.60	1.59	4.11
Sum	4610	100.00			

Preparative separation for compound **Pt1**

• Sample preparation: About 20 mg of compound was dissolved in 3.5 mL of dichloromethane.

• Chromatographic conditions: Chiralpak IA (250 x 10 mm), hexane / 2-PrOH / dichloromethane (85/5/10) as mobile phase, flow-rate = 5 mL/min, UV detection at 254 nm.

• Injections (stacked): 14 times 250 μL, every 10 minutes.

First fraction: 3.8 mg of the first eluted with *ee* > 99%:

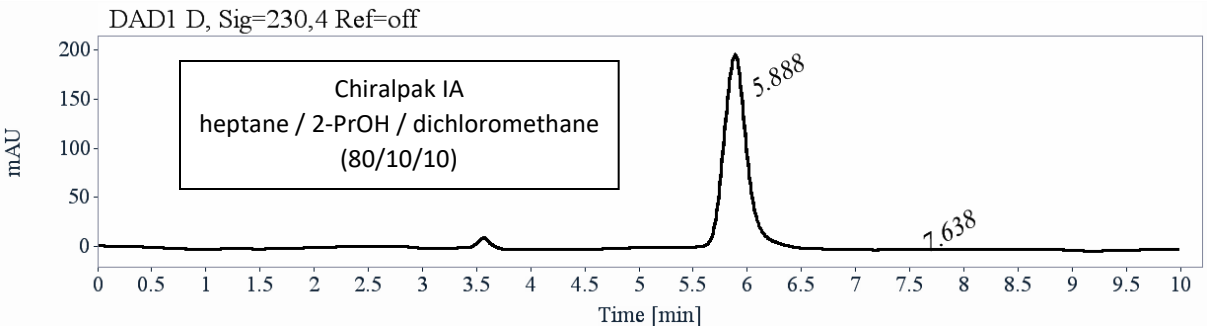

RT [min]	Area	Area%
5.89	2897	99.71
7.64	9	0.29
Sum	2906	100.00

Second fraction: 4.6 mg of the second eluted with *ee* > 98%:

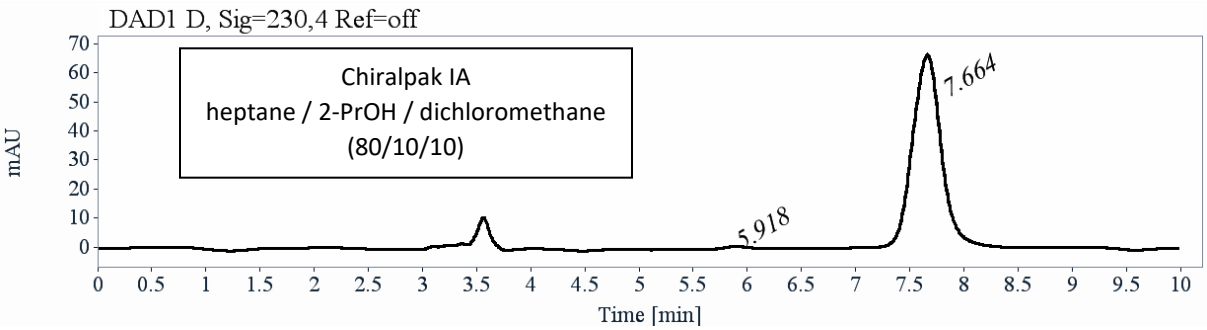

RT [min]	Area	Area%
5.92	10	0.82
7.66	1232	99.18
Sum	1242	100.00

Analytical chiral HPLC separation for compound **Pt2**

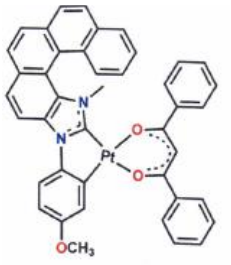

• The sample is dissolved in dichloromethane, injected on the chiral column, and detected with a UV detector at 230 nm and a circular dichroism detector at 254 nm. The flow-rate is 1 mL/min.

Column	Mobile Phase	t1	k1	t2	k2	α	Rs
Chiralpak IF	heptane / ethanol / dichloromethane (60/20/20)	6.34	1.15	8.54	1.90	1.65	5.20

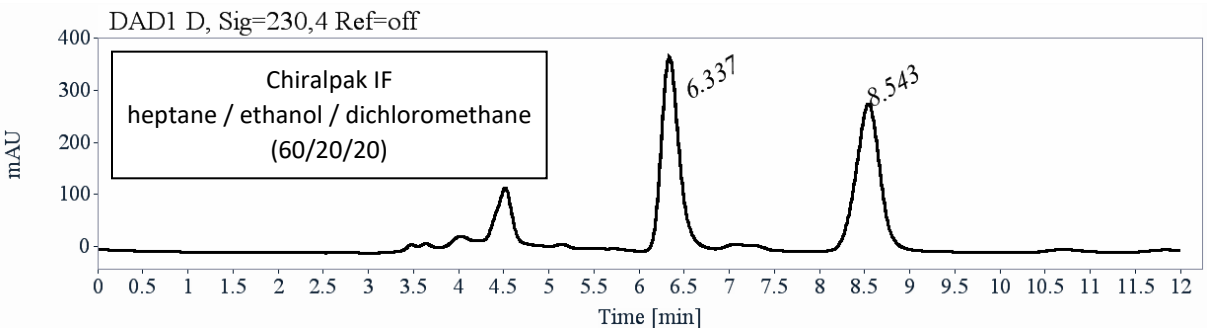

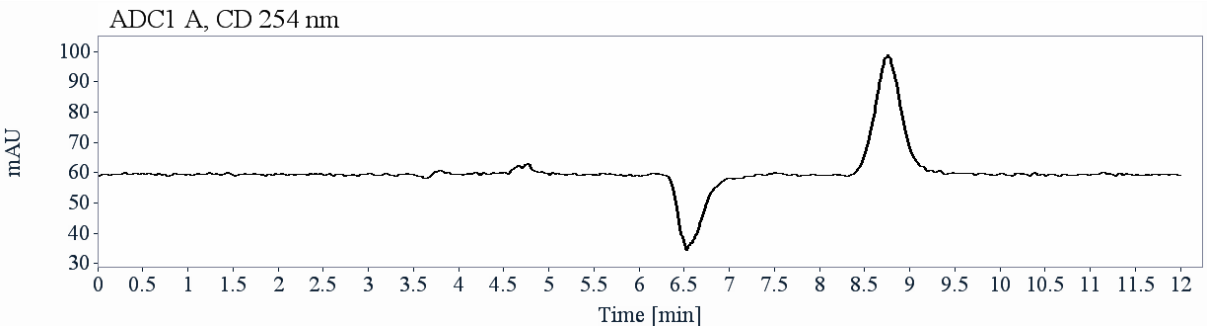

RT [min]	Area	Area%	Capacity Factor	Enantioselectivity	Resolution (USP)
6.34	5055	48.73	1.15		
8.54	5318	51.27	1.90	1.65	5.20
Sum	10373	100.00			

Preparative separation for compound **Pt2**

• Sample preparation: About 50 mg of compound was dissolved in 8.8 mL of dichloromethane / ethanol / hexane = 75/5/20.

• Chromatographic conditions: Chiralpak IF (250 x 10 mm), hexane / ethanol / dichloromethane (50/20/20) as mobile phase, flow-rate = 5 mL/min, UV detection at 254 nm.

• Injections (stacked): 35 times 250 μL, every 9.5 minutes.

First fraction: 14 mg of the first eluted with *ee* > 99.5%:

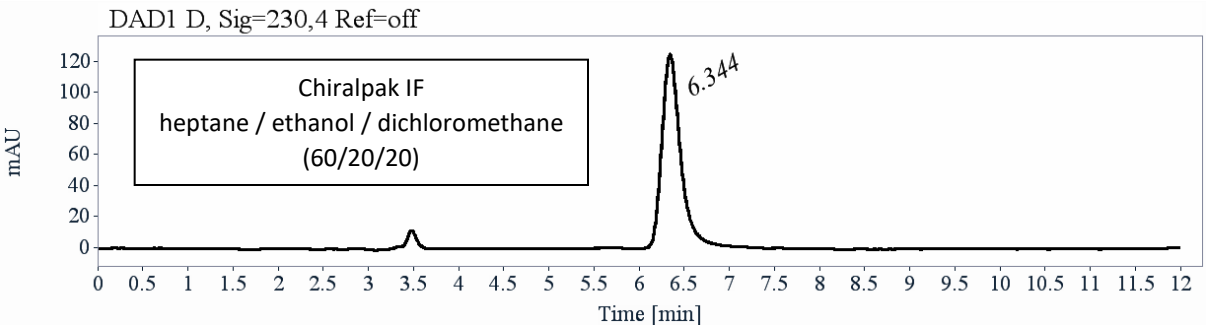

RT [min]	Area	Area%
6.34	1772	100.00
Sum	1772	100.00

Second fraction: 14 mg of the second eluted with *ee* > 99.5%:

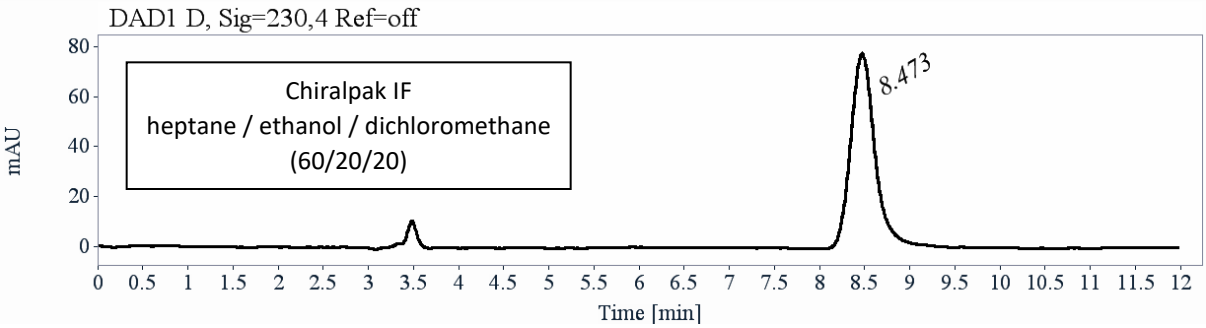

RT [min]	Area	Area%
8.47	1482	100.00
Sum	1482	100.00

S1.6. X-ray crystallographic data

The data were collected at low temperature (150 K) on an APEXII Bruker-AXS diffractometer equipped with a CCD-LDI-APEX2 detector, using MoKα radiation (λ = 0.71073 Å). The structure was solved using SHELXT 2018_2. All non-hydrogen atoms were refined with SHELXL-2018.

Table S1.1: *X-ray crystallographic data for (rac)-**Pt2**•CH_2Cl_2.*

	(*rac*)-Pt2•CH_2Cl_2
Empirical Formula	$C_{43}H_{32}Cl_2N_2O_3Pt$
CCDC number	2207037
Formula Weight	890.69
Temperature (K)	150
Wavelenght (Å)	0.71073
Crystal system	Triclinic
Space Group	*P*-1
a (Å)	10.1129(8)
b (Å)	13.0517(10)
c (Å)	13.8906(9)
α (°)	77.079(2)
β (°)	73.709(2)
γ (°)	85.307(2)
Volume (Å^3)	1714.9(2)
Z	2
Color	Yellow
$d_{calculated}$ (g·cm^{-3})	1.725
Absorption coefficient (mm^{-1})	4.293
Tmin	0.213
Tmax	0.357
F (000)	880
Crystal size (mm)	0.700 x 0.280 x 0.240
Θ range for data collection (°)	2.614 to 27.515
Limiting indices	-13 ≤ h ≤ 13 -16 ≤ k ≤ 14 -18 ≤ l ≤ 13
Data completeness	97.8 %
Reflection collected	23231
Reflections uniques	7713 [R(int) = 0.0517]
Data / restraints / parameters	7713 / 0 / 462
Goodness-on-fit on F^2	1.009
Final *R* indices [I > 2σ]	R1 = 0.0310, wR2 = 0.0591
R indices (all data)	R1 = 0.0380, wR2 = 0.0613
Largest diff peak and hole (eÅ^{-3})	1.146 and -1.006

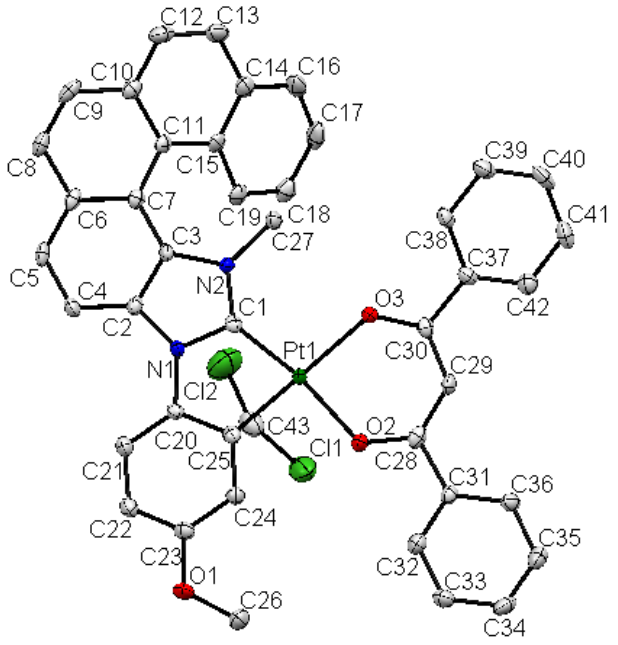

Figure S1.12: *ORTEP figure (thermal ellipsoids represent 50% probability) from X-ray diffraction experiment for (rac)-**Pt2**•CH_2Cl_2. Hydrogen atoms are omitted for clarity.*

S1.7. Photophysical and chiroptical measurements

Optical rotations

The specific optical rotation values for the (*P*) and (*M*) enantiomers of complexes **Pt1** and **Pt2** were measured in toluene (*C* = 1.2 mg/mL for **Pt1** and 1 mg/mL for **Pt2**) at room temperature.

Table S1.2: *Specific optical rotation values of **Pt1** and **Pt2** in toluene at 298 K.*

	(*P*)-(+)-Pt1	**(*M*)-(-)-Pt1**	**(*P*)-(+)-Pt2**	**(*M*)-(-)-Pt2**
$[\alpha]_{589}^{25}$	+952	-947	+755	-742

Absorption and ECD measurements

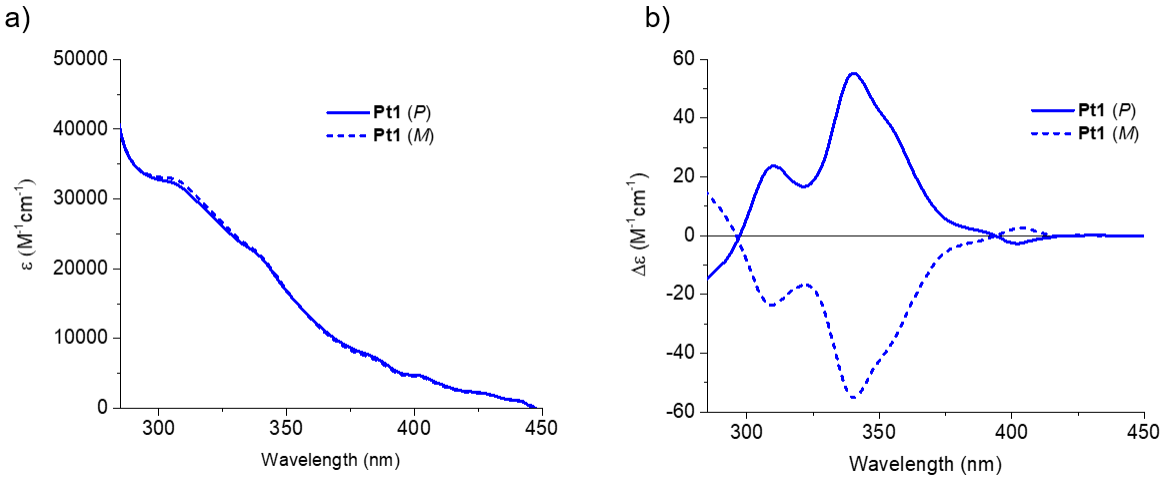

Figure S1.13: *a) UV-vis and b) ECD spectra of* ***Pt1*** *enantiomers in toluene at room temperature (C = 2 × 10^{-5} M).*

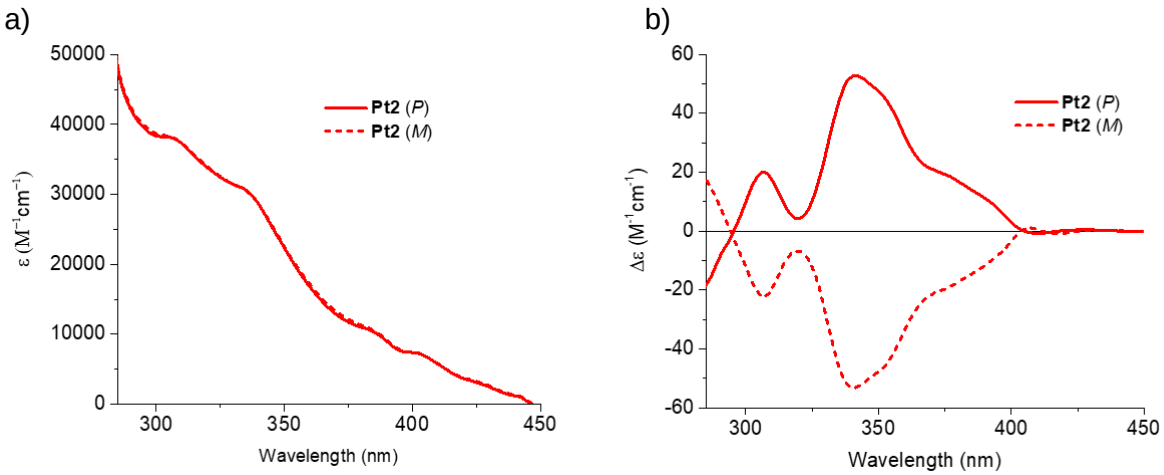

Figure S1.14: *a) UV-vis and b) ECD spectra of* ***Pt2*** *enantiomers in toluene at room temperature (C = 2 × 10^{-5} M).*

Luminescence

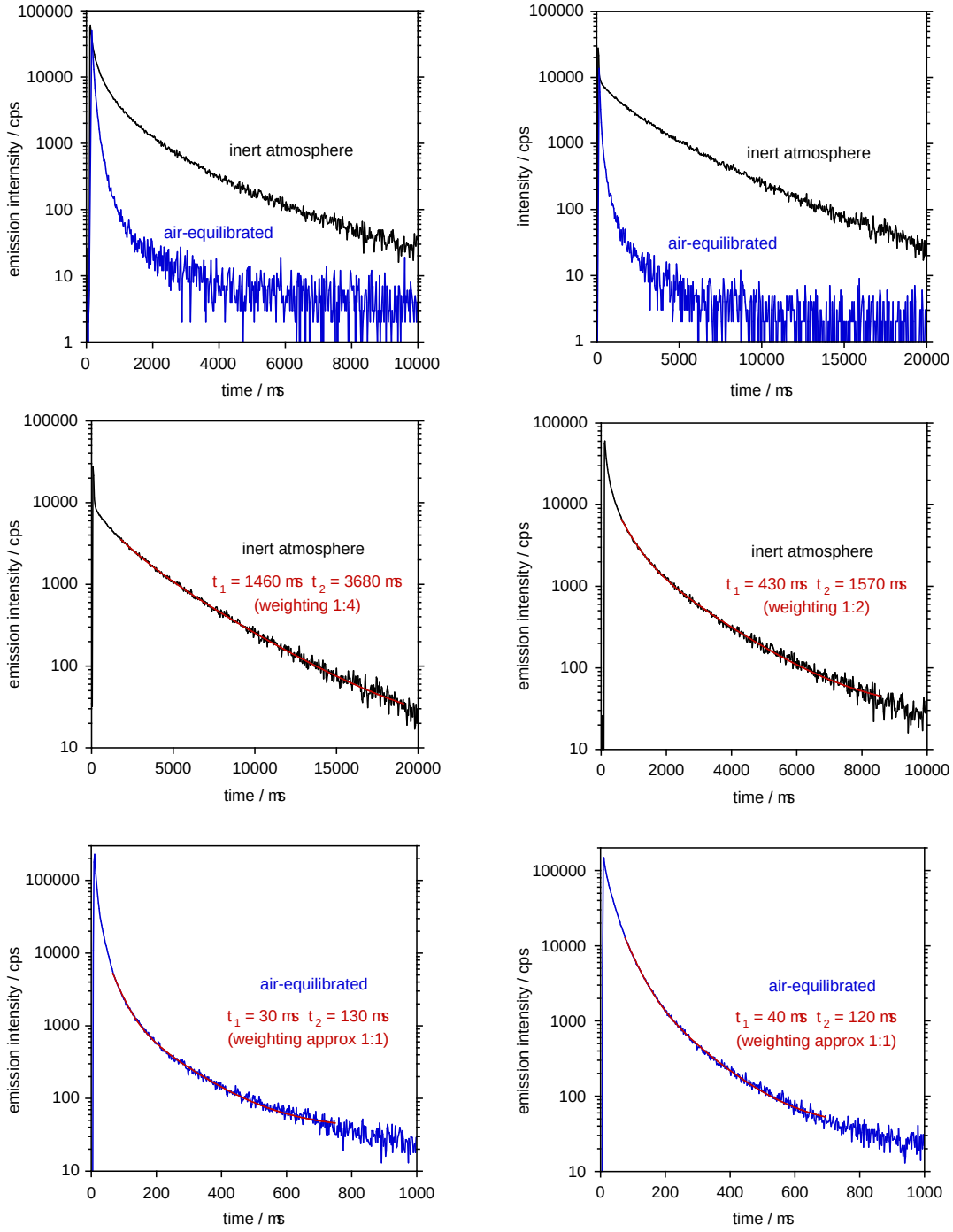

Figure S1.15: *Luminescence decay kinetics of* ***Pt1*** *(left) and* ***Pt2*** *(right) at 2 wt% in PMMA at 295 K.* ***Top:*** *Decays under inert atmosphere (black) and the corresponding traces under air-equilibrated conditions (blue) shown on the same timescale for comparison.* ***Middle:*** *The decays under inert atmosphere (black), fitted to a sum of two exponentials as shown in red.* ***Bottom:*** *The decays under air-equilibrated conditions (blue), fitted to a sum of two exponentials as shown in red.*

CPL measurements

The parameters were: excitation wavelength = 365 nm, emission bandwidth ~ 10 nm, integration time = 4 sec, scan-speed = 50 nm/min, accumulations = 3.

The reported spectra are normalized on the maximum of their corresponding photoluminescence spectra, so that the g_{lum} values can be directly read on the *y*-axis at the maximum of each curve.

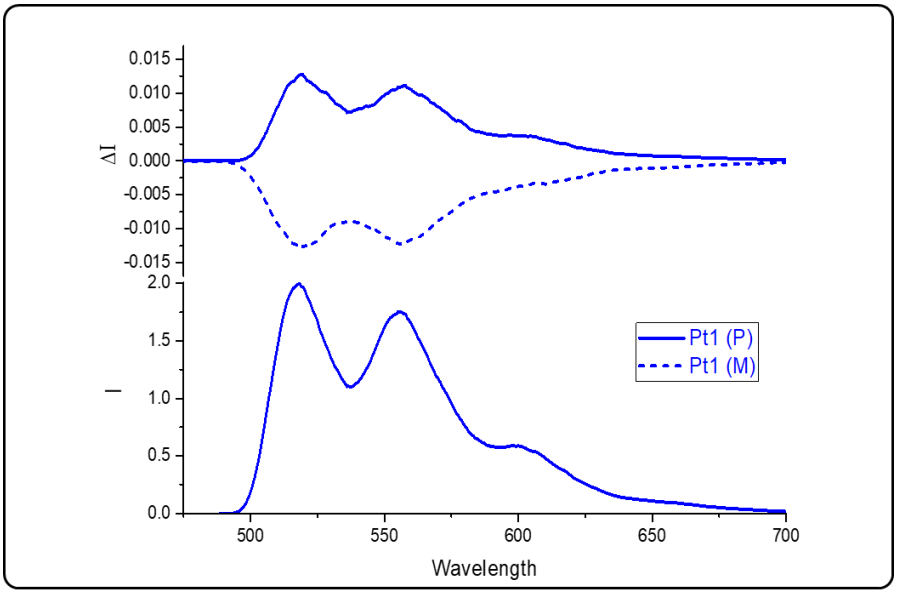

Figure S1.16: *CPL spectra of enantiomeric pair of (P)- and (M)-**Pt1** measured in 2-methyl-THF at 77 K (λ_{ex}= 365 nm) (top) along with the corresponding photoluminescence spectra (bottom).*

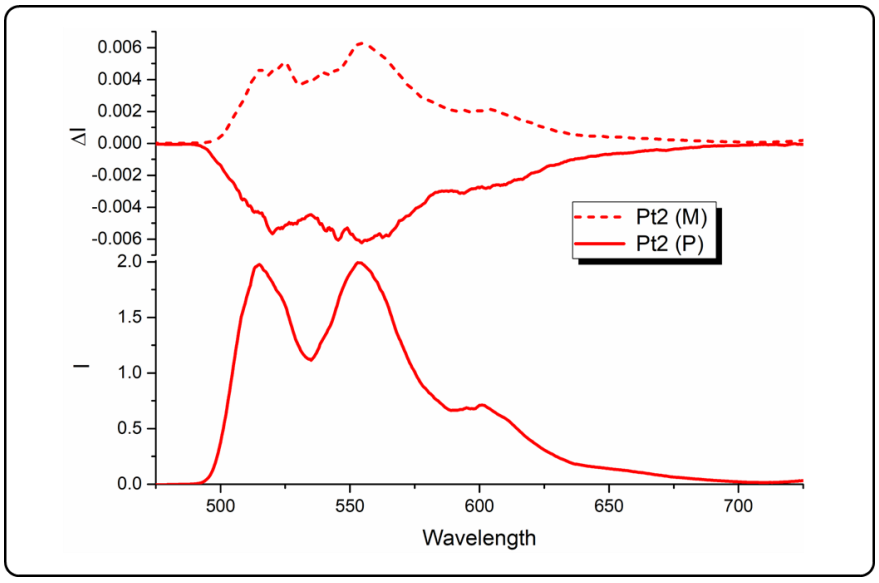

Figure S1.17: *CPL spectra of enantiomeric pair of (P)- and (M)-**Pt2** measured in 2-methyl-THF at 77 K (λ_{ex}= 365 nm) (top) along with the corresponding photoluminescence spectra (bottom).*

S2. Computational section

S2.1. Computational details

The computational protocol employed in the presented study follows that used in References [2a,3] to successfully characterize Ir(III)- and Re(I)-based complexes comprising NHC-[5]helicene ligands. All the calculations were performed with the Gaussian 16 (G16) program,[4] utilizing SV(P)[5] basis set for lighter atoms (H, C, N, O) and the SDD (Stuttgart/Dresden RSC 1997) basis and the matching 60-electron scalar relativistic effective core potential for the metal (Pt).[6,7] Solvent effects were considered by means of the polarizable continuum model (PCM)[8,9,10,11,12] for toluene (ε = 2.3741) and tetrahydrofuran (THF, ε = 7.4257); note that THF was used to approximate 2-methyl-tetrahydrofuran solvent that was experimentally employed in low-temperature emission measurements but parameters of which are not implemented in G16. No symmetry was explicitly imposed in the computations.

Geometry optimizations of the studied Pt(II) complexes **Pt1** and **Pt2** were performed employing density functional theory (DFT) approach with the B3LYP exchange-correlation functional.[13,14,15] For **Pt2**, different rotameric structures for phenyl groups in dibenzoylmethane moiety were considered (see Figure S2.1).

Optical rotation (OR) parameters, absorption and electronic circular dichroism (ECD) spectra were modelled via time-dependent DFT (TDDFT) linear response calculations. The sodium-D line (λ = 589.3 nm) ORs were computed with the BHLYP[15,16] and PBE0[17,18] functionals, the former demonstrating a better agreement with the experimental data (Table S2.1). Absorption UV-vis and ECD spectra were simulated based on calculations of the lowest 120 vertical singlet electronic excitations, followed by Gaussian broadening of the intensities using the GaussView 5.0.9 program.[19] The Gaussian broadening parameter was chosen to be σ = 0.20 eV for all the spectra. This subset of computations employed the PBE0 functional, and some benchmark calculations were also performed with CAM-B3LYP[20] which however did not show any improved agreement with experiments (Figure S2.2). Accordingly, the assignments of the spectra were thus based on an analysis of the PBE0 results.

Electronic emission (phosphorescence) spectra via T_1 excited-states geometry optimizations were modelled using the TDDFT-PBE0 approach with the Tamm-Dancoff approximation (TDA).[21,22,23,24,25,26] Some benchmark calculations were also performed not employing the TDA but in most cases they were found to underestimate the T_1 energies significantly, in line with the previous observation for some helicene-based metal complexes.[27,28,29,30] Importantly, however, both corresponding sets of computations (with and without the TDA) show overall the same electronic assignment of the T_1-S_0 emission transitions. For the optimized T_1 excited-state structures of **Pt2**, frequencies calculations were performed at the corresponding level of theory in order to confirm that they all represent energy minima (no imaginary frequencies) on T_1 excited-state potential energy surface.

S2.2. Additional calculated data

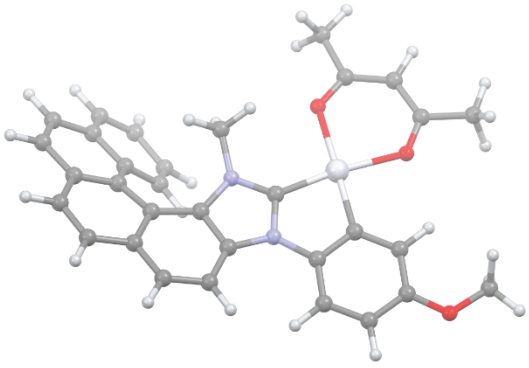

(*P*)-**Pt1**

(*P*)-**Pt2-I**

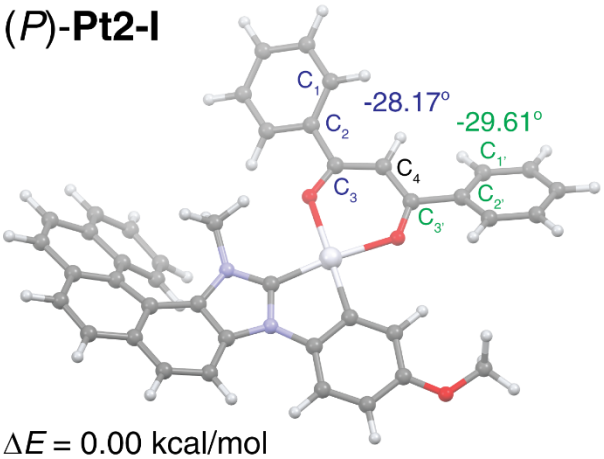

ΔE = 0.00 kcal/mol
n_B = 33.1%

(*P*)-**Pt2-II**

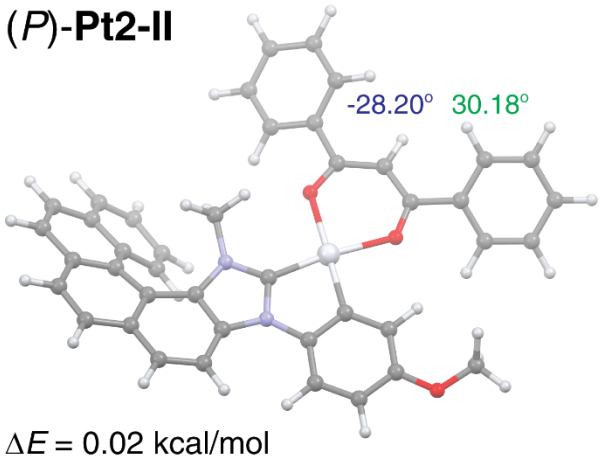

ΔE = 0.02 kcal/mol
n_B = 32.2%

(*P*)-**Pt2-III**

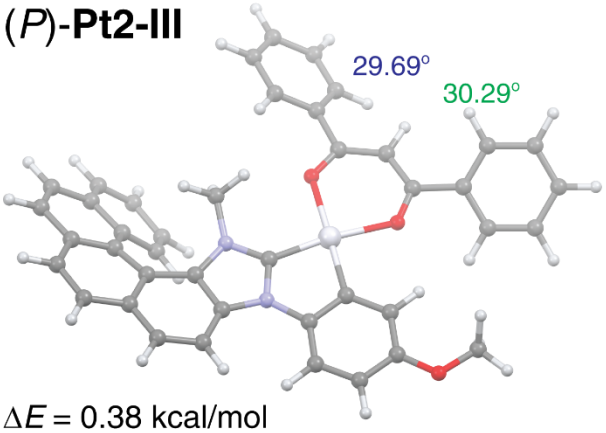

ΔE = 0.38 kcal/mol
n_B = 17.5%

(*P*)-**Pt2-IV**

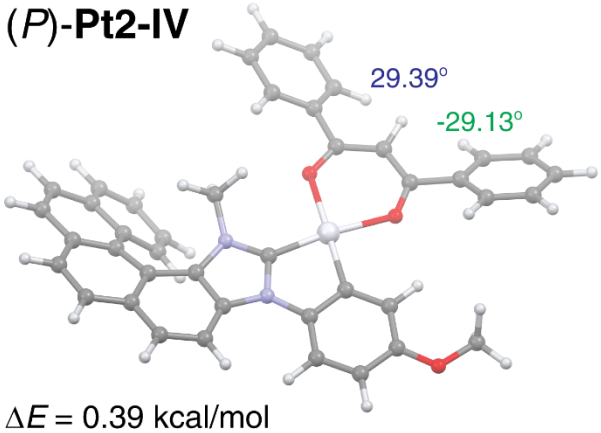

ΔE = 0.39 kcal/mol
n_B = 17.2%

Figure S2.1: *Optimized (DFT-B3LYP//SDD/SV(P) with continuum solvent model for toluene) structures of helicene-NHC-Pt complexes* ***Pt1*** *and* ***Pt2****. Values listed for* ***Pt2*** *are dihedral angles (as defined on the structure* ***Pt2-I****), relative energies ΔE and the corresponding Boltzmann populations (at 25 °C)* n_B*. Note that (P)-****Pt2-IV*** *structure corresponds to that found in the X-ray crystal structure of the compound.*

Table S2.1: *Experimental and calculated specific optical rotations* $[\alpha]_D$ *(in* 10^{-1} *deg·cm²·g⁻¹) of helicene-NHC-Pt complexes (P)-**Pt1** and (P)-**Pt2**.*

Method	(*P*)-**Pt1**	(*P*)-**Pt2** [a]				
		I	**II**	**III**	**IV**	**averd.**
BHLYP//SDD/SV(P) PCM(toluene)	940.2	606.6	918.1	1153	846.7	843.8
PBE0//SDD/SV(P) PCM(toluene)	1296	920.7	1306	1601	1219	1215
Expt. (25 °C)	952 (-947)[b]			755 (-742)[b]		

[a] Numbers listed (I, II, III, IV) correspond to different **Pt2** conformers (see Figure S2.1), 'averd.' indicates Boltzmann-averaged value at 25 °C. [b] Value for (*M*) enantiomer.

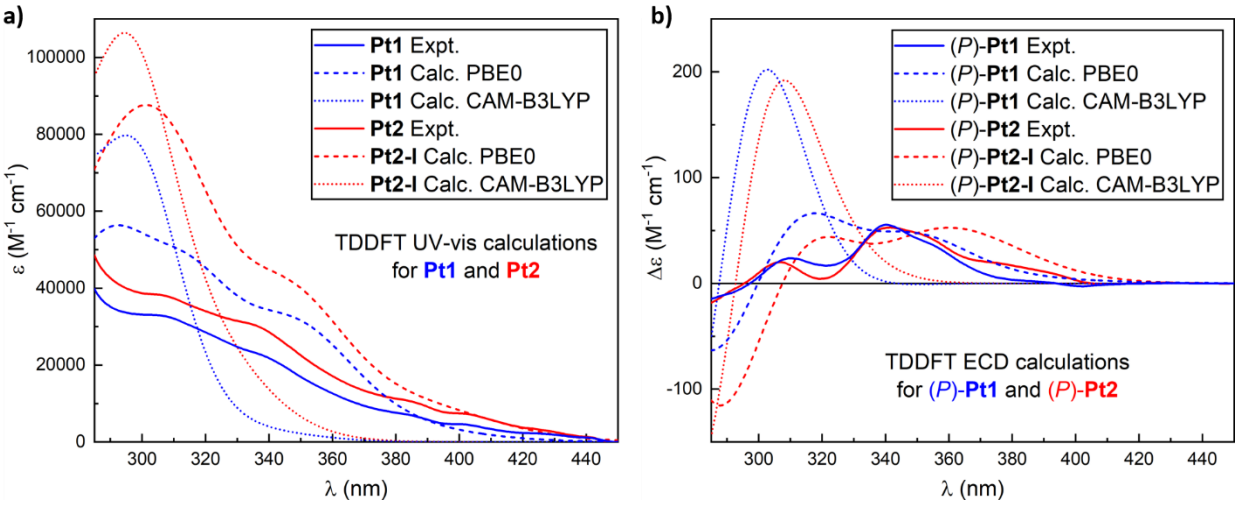

Figure S2.2: *Experimental and simulated (TDDFT-PBE0//SDD/SV(P) and TDDFT-CAM-B3LYP//SDD/SV(P) with continuum solvent model for toluene) UV-vis (panel a) and ECD (panel b) spectra for helicene-NHC-Pt complexes **Pt1** and **Pt2** (conformer I, see Figure S2.1 for structure visualization).*

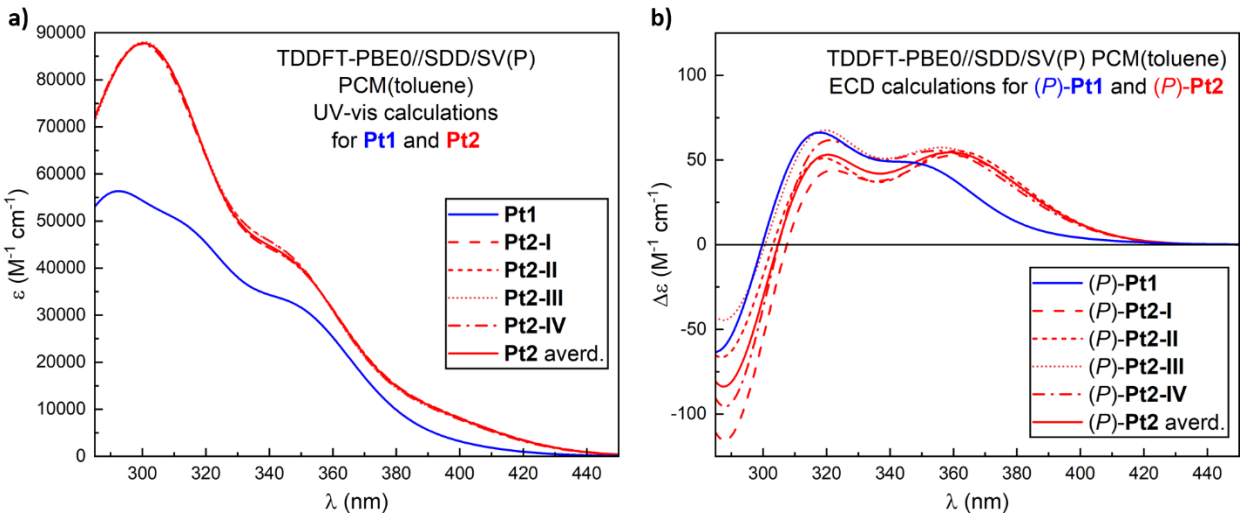

Figure S2.3: *Simulated (TDDFT-PBE0//SDD/SV(P) with continuum solvent model for toluene) UV-vis (panel a) and ECD (panel b) spectra for helicene-NHC-Pt complexes **Pt1** and **Pt2** (conformers I-IV, see Figure S2.1 for structures visualization; 'averd.' corresponds to Boltzmann-averaged (25 °C) spectrum).*

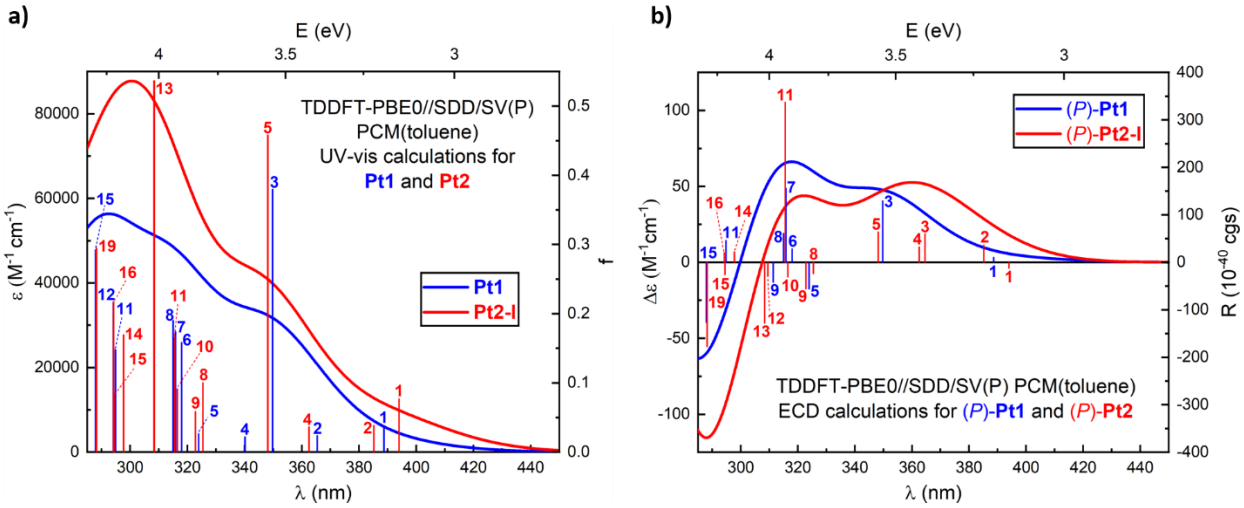

Figure S2.4: *Simulated (TDDFT-PBE0//SDD/SV(P) with continuum solvent model for toluene) UV-vis (panel a) and ECD (panel b) spectra for helicene-NHC-Pt complexes **Pt1** and **Pt2** (conformer I, see Figure S2.1 for structure visualization). No spectral shift has been applied. Selected calculated excitation energies along with the corresponding oscillator and rotatory strengths, analyzed in detail (see Tables S2.2 and S2.3 and Figures S2.6 and S2.7), indicated as 'stick' spectra.*

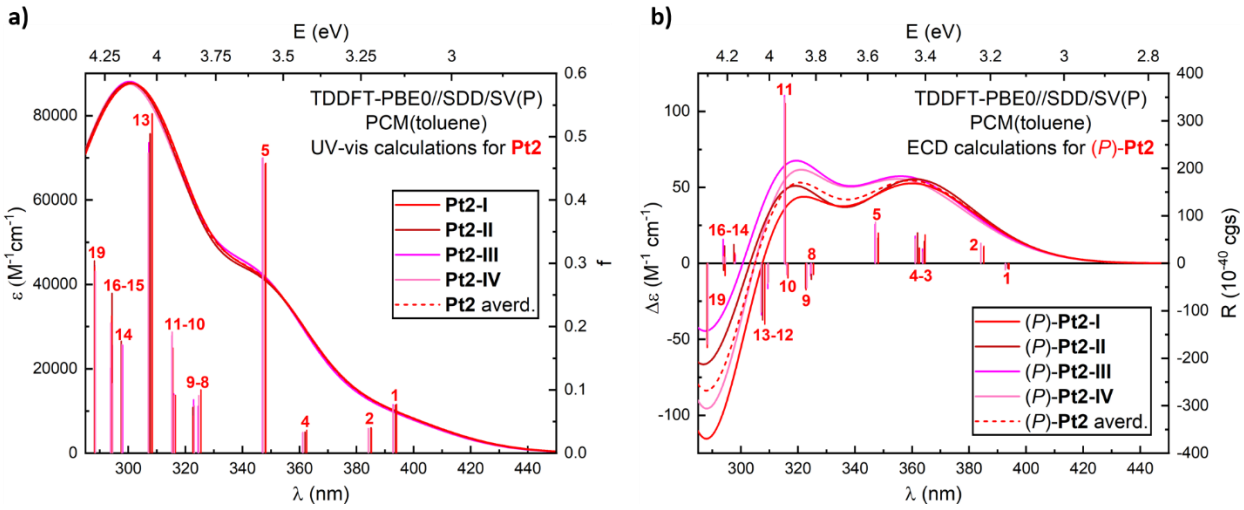

Figure S2.5: *Simulated (TDDFT-PBE0//SDD/SV(P) with continuum solvent model for toluene) UV-vis (panel a) and ECD (panel b) spectra for different conformers (I-IV, see Figure S2.1 for structures visualization) of helicene-NHC-Pt complex* ***Pt2****. 'averd.' corresponds to Boltzmann-averaged (25 °C) spectrum. No spectral shift has been applied. Selected calculated excitation energies along with the corresponding oscillator and rotatory strengths, analyzed in detail (see Tables S2.3-S2.6 and Figure S2.7), indicated as 'stick' spectra.*

Table S2.2: *Selected dominant excitations and occupied (occ) – unoccupied (unocc) MO-pair contributions (greater than 10%) for helicene-NHC-Pt complex* ***Pt1****. For MOs visualization, see Figure S2.6. Based on TDDFT-PBE0//SDD/SV(P) with continuum solvent model for toluene calculations.*

Excitation	*E* / eV	λ / nm	*f*	*R* / 10^{-40} cgs	occ no.	unocc no.	%	Assignment
1	3.190	389	0.035	10.44	137	138	86.4	anisole-NHC-Pt→NHC-helicene (IL- & ML-CT)
2	3.393	365	0.024	-5.10	137	139	64.8	anisole-NHC-Pt→NHC-helicene (IL- & ML-CT)
					136	138	23.2	NHC-helicene-Pt-acac→NHC-helicene (π-π* & LL- & ML-CT)
3	3.545	350	0.379	129.38	136	138	39.7	NHC-helicene-Pt-acac→NHC-helicene (π-π* & LL- & ML-CT)
					136	139	21.2	NHC-helicene-Pt-acac→NHC-helicene (π-π* & LL- & ML-CT)

					137	139	17.5	anisole-NHC-Pt→NHC-helicene (IL- & ML-CT)
4	3.645	340	0.022	-1.45	136	139	32.6	NHC-helicene-Pt-acac→NHC-helicene (π-π* & LL- & ML-CT)
					136	138	22.7	NHC-helicene-Pt-acac→NHC-helicene (π-π* & LL- & ML-CT)
					135	138	15.1	anisole-NHC-helicene-Pt-acac→NHC-helicene (π-π* & IL- & LL- & ML-CT)
5	3.827	324	0.026	-55.70	137	141	44.8	anisole-NHC-Pt→anisole-NHC-helicene-Pt-acac (π-π* & MM & IL- & LL- & ML-CT)
					137	140	15.3	anisole-NHC-Pt→acac (LL- / ML-CT)
					136	139	10.0	NHC-helicene-Pt-acac→NHC-helicene (π-π* & LL- & ML-CT)
6	3.899	318	0.158	28.54	135	138	54.8	anisole-NHC-helicene-Pt-acac→NHC-helicene (π-π* & IL- & LL- & ML-CT)
					137	141	16.6	anisole-NHC-Pt→anisole-NHC-helicene-Pt-acac (π-π* & MM & IL- & LL- & ML-CT)
7	3.926	316	0.174	156.04	135	139	19.3	anisole-NHC-helicene-Pt-acac→NHC-helicene (π-π* & IL- & LL- & ML-CT)
					133	138	18.7	helicene-anisole-Pt→NHC-helicene (π-π* & IL- & ML-CT)
					137	140	17.7	anisole-NHC-Pt→acac (LL- / ML-CT)
					136	139	15.4	NHC-helicene-Pt-acac→NHC-helicene (π-π* & LL- & ML-CT)
8	3.936	315	0.190	61.10	137	140	49.9	anisole-NHC-Pt→acac (LL- / ML-CT)

					135	138	17.2	anisole-NHC-helicene-Pt-acac→NHC-helicene (π-π^* & IL- & LL- & ML-CT)
9	3.983	311	0.016	-41.84	134	138	39.1	Pt(d_{z2})→NHC-helicene (ML-CT)
					134	139	22.7	Pt(d_{z2})→NHC-helicene (ML-CT)
					134	141	16.3	Pt(d_{z2})→anisole-NHC-helicene-Pt-acac (MM & ML-CT)
11	4.205	295	0.148	46.03	133	138	38.3	helicene-anisole-Pt→NHC-helicene (π-π^* & IL- & ML-CT)
					135	139	30.9	anisole-NHC-helicene-Pt-acac→NHC-helicene (π-π^* & IL- & LL- & ML-CT)
12	4.216	294	0.217	-0.42	133	139	25.7	helicene-anisole-Pt→NHC-helicene (π-π^* & IL- & ML-CT)
					132	138	19.2	anisole-Pt-acac→NHC-helicene (IL- / LL- / ML-CT)
					135	139	17.0	anisole-NHC-helicene-Pt-acac→NHC-helicene (π-π^* & IL- & LL- & ML-CT)
15	4.306	288	0.288	-126.52	136	141	53.7	NHC-helicene-Pt-acac→anisole-NHC-helicene-Pt-acac (π-π^* & MM & IL- & LL- & ML-CT)
					136	140	13.8	NHC-helicene-Pt-acac→acac (π-π^* & LL- & ML-CT)
					133	138	10.5	helicene-anisole-Pt→NHC-helicene (π-π^* & IL- & ML-CT)

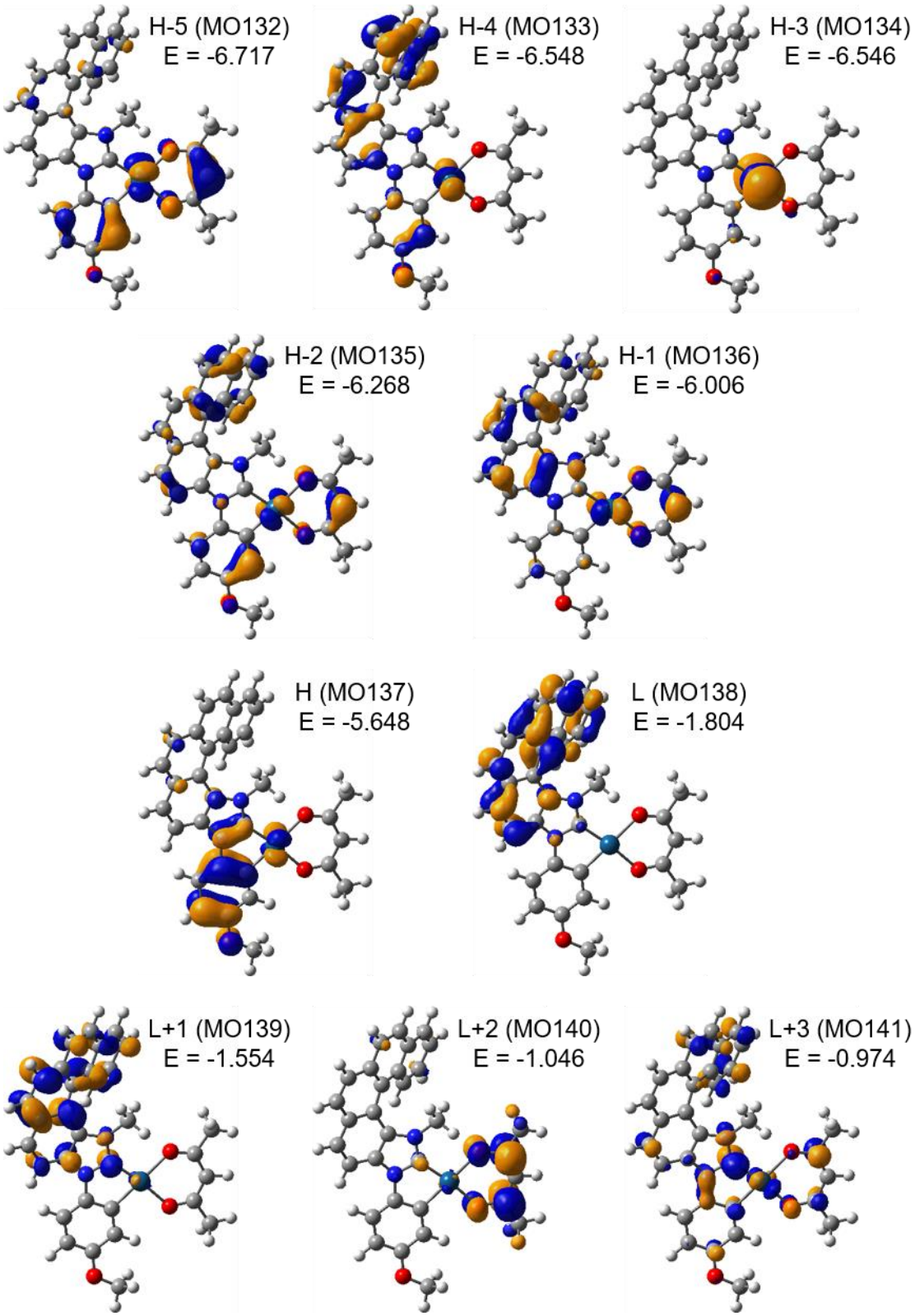

Figure S2.6: *Isosurfaces (±0.04 au) of MOs involved in selected electronic transitions of* ***Pt1****. Based on PBE0//SDD/SV(P) with continuum solvent model for toluene calculations. H = HOMO, L = LUMO. Values E listed are orbital energies, in eV.*

Table S2.3: *Selected dominant excitations and occupied (occ) – unoccupied (unocc) MO-pair contributions (greater than 10%) for helicene-NHC-Pt complex* ***Pt2-I****. For MOs visualization, see Figure S2.7. Based on TDDFT-PBE0//SDD/SV(P) with continuum solvent model for toluene calculations.*

Excitation	*E* / eV	λ / nm	*f*	*R* / 10^{-40} cgs	occ no.	unocc no.	%	Assignment
1	3.147	394	0.077	-12.19	169	170	88.0	anisole-NHC-Pt→dbm (LL- & ML-CT)
2	3.219	385	0.039	36.17	169	171	80.7	anisole-NHC-Pt→NHC-helicene (IL- & ML-CT)
3	3.401	365	0.003	60.03	169	172	46.0	anisole-NHC-Pt→NHC-helicene (IL- & ML-CT)
					168	171	19.3	NHC-helicene-Pt-dbm_{core}→NHC-helicene (π-π* & LL- & ML-CT)
					168	170	18.2	NHC-helicene-Pt-dbm_{core}→dbm (π-π* & IL- & LL- & ML-CT)
4	3.420	362	0.037	32.43	168	170	65.2	NHC-helicene-Pt-dbm_{core}→dbm (π-π* & IL- & LL- & ML-CT)
					169	172	15.6	anisole-NHC-Pt→NHC-helicene (IL- & ML-CT)
5	3.562	348	0.458	63.74	168	171	30.0	NHC-helicene-Pt-dbm_{core}→NHC-helicene (π-π* & LL- & ML-CT)
					168	172	23.5	NHC-helicene-Pt-dbm_{core}→NHC-helicene (π-π* & LL- & ML-CT)
					169	172	19.7	anisole-NHC-Pt→NHC-helicene (IL- & ML-CT)
8	3.810	325	0.100	-23.74	167	170	75.4	anisole-NHC-helicene-Pt-dbm_{core}→dbm (π-π* & IL- & LL- & ML-CT)
9	3.841	323	0.059	-55.73	169	173	58.7	anisole-NHC-Pt→anisole-NHC-helicene-Pt (π-π* & MM & IL- & ML-CT)
10	3.918	316	0.091	-31.10	167	171	49.2	anisole-NHC-helicene-Pt-dbm_{core}→NHC-helicene

								(π-π* & IL- & LL- & ML-CT)
					167	172	15.8	anisole-NHC-helicene-Pt-dbm_{core}→NHC-helicene (π-π* & IL- & LL- & ML-CT)
11	3.929	316	0.166	337.07	168	172	22.7	NHC-helicene-Pt-dbm_{core}→NHC-helicene (π-π* & LL- & ML-CT)
					167	171	20.3	anisole-NHC-helicene-Pt-dbm_{core}→NHC-helicene (π-π* & IL- & LL- & ML-CT)
					166	171	16.8	helicene-anisole-Pt→NHC-helicene (π-π* & IL- & ML-CT)
12	4.006	309	0.012	-29.60	165	171	39.9	Pt(d_{z2})→NHC-helicene (ML-CT)
					165	172	27.8	Pt(d_{z2})→NHC-helicene (ML-CT)
					165	173	22.7	Pt(d_{z2})→anisole-NHC-helicene-Pt (MM & ML-CT)
13	4.021	308	0.536	-128.08	164	170	76.2	anisole-Pt-dbm→dbm (π-π* & IL- & LL- & ML-CT)
14	4.165	298	0.169	21.92	166	170	69.2	helicene-anisole-Pt→dbm (LL- & ML-CT)
15	4.211	294	0.085	-25.96	162	170	39.4	Pt-dbm→dbm (π-π* & IL- & ML-CT)
16	4.215	294	0.217	20.16	167	172	39.5	anisole-NHC-helicene-Pt-dbm_{core}→NHC-helicene (π-π* & IL- & LL- & ML-CT)
					166	171	16.7	helicene-anisole-Pt→NHC-helicene (π-π* & IL- & ML-CT)
					162	170	12.4	Pt-dbm→dbm (π-π* & IL- & ML-CT)
19	4.302	288	0.295	-177.78	168	173	60.1	NHC-helicene-Pt-dbm_{core}→ anisole-NHC-helicene-Pt (π-π* & MM & IL- & LL- & ML-CT)
					166	171	16.2	helicene-anisole-Pt→NHC-helicene (π-π* & IL- & ML-CT)

Table S2.4: *Selected dominant excitations and occupied (occ) – unoccupied (unocc) MO-pair contributions (greater than 10%) for helicene-NHC-Pt complex* ***Pt2-II****. For MOs visualization, see Figure S2.7. Based on TDDFT-PBE0//SDD/SV(P) with continuum solvent model for toluene calculations.*

Excitation	*E* / eV	λ / nm	*f*	*R* / 10^{-40} cgs	occ no.	unocc no.	%	Assignment
1	3.150	394	0.076	-11.02	169	170	86.9	anisole-NHC-Pt→dbm (LL- & ML-CT)
2	3.220	385	0.040	33.74	169	171	80.2	anisole-NHC-Pt→NHC-helicene (IL- & ML-CT)
3	3.403	364	0.005	46.52	169	172	52.4	anisole-NHC-Pt→NHC-helicene (IL- & ML-CT)
					168	171	21.7	NHC-helicene-Pt-dbm_{core}→NHC-helicene (π-π* & LL- & ML-CT)
4	3.426	362	0.033	64.34	168	170	73.3	NHC-helicene-Pt-dbm_{core}→dbm (π-π* & IL- & LL- & ML-CT)
5	3.563	348	0.457	53.23	168	171	29.9	NHC-helicene-Pt-dbm_{core}→NHC-helicene (π-π* & LL- & ML-CT)
					168	172	23.5	NHC-helicene-Pt-dbm_{core}→NHC-helicene (π-π* & LL- & ML-CT)
					169	172	19.7	anisole-NHC-Pt→NHC-helicene (IL- & ML-CT)
8	3.819	325	0.080	-34.00	167	170	68.1	anisole-NHC-helicene-Pt-dbm_{core}→dbm (π-π* & IL- & LL- & ML-CT)
9	3.843	323	0.073	-52.41	169	173	55.0	anisole-NHC-Pt→anisole-NHC-helicene-Pt (π-π* & MM & IL- & ML-CT)
10	3.920	316	0.091	-2.08	167	171	49.9	anisole-NHC-helicene-Pt-dbm_{core}→NHC-helicene (π-π* & IL- & LL- & ML-CT)
					167	172	15.8	anisole-NHC-helicene-Pt-dbm_{core}→NHC-helicene (π-π* & IL- & LL- & ML-CT)
11	3.932	315	0.186	325.10	168	172	24.0	NHC-helicene-Pt-dbm_{core}→NHC-helicene

								(π-π* & LL- & ML-CT)
					167	171	20.2	anisole-NHC-helicene-Pt-dbm_{core}→NHC-helicene (π-π* & IL- & LL- & ML-CT)
					166	171	16.6	helicene-anisole-Pt→NHC-helicene (π-π* & IL- & ML-CT)
12	4.005	310	0.013	-39.81	165	171	37.7	$Pt(d_{z2})$→NHC-helicene (ML-CT)
					165	172	26.0	$Pt(d_{z2})$→NHC-helicene (ML-CT)
					165	173	21.8	$Pt(d_{z2})$→anisole-NHC-helicene-Pt (MM & ML-CT)
13	4.031	308	0.505	-119.55	164	170	77.1	anisole-Pt-dbm→dbm (π-π* & IL- & LL- & ML-CT)
14	4.167	298	0.177	39.91	166	170	66.5	helicene-anisole-Pt→dbm (LL- & ML-CT)
15	4.213	294	0.253	36.90	167	172	40.8	anisole-NHC-helicene-Pt-dbm_{core}→NHC-helicene (π-π* & IL- & LL- & ML-CT)
					166	171	16.9	helicene-anisole-Pt→NHC-helicene (π-π* & IL- & ML-CT)
19	4.303	288	0.304	-159.44	168	173	61.2	NHC-helicene-Pt-dbm_{core}→anisole-NHC-helicene-Pt (π-π* & MM & IL- & LL- & ML-CT)
					166	171	15.9	helicene-anisole-Pt→NHC-helicene (π-π* & IL- & ML-CT)

Table S2.5: *Selected dominant excitations and occupied (occ) – unoccupied (unocc) MO-pair contributions (greater than 10%) for helicene-NHC-Pt complex* ***Pt2-III****. For MOs visualization, see Figure S2.7. Based on TDDFT-PBE0//SDD/SV(P) with continuum solvent model for toluene calculations.*

Excitation	*E* / eV	λ / nm	*f*	*R* / 10^{-40} cgs	occ no.	unocc no.	%	Assignment
1	3.157	393	0.077	-11.16	169	170	86.7	anisole-NHC-Pt→dbm (LL- & ML-CT)
2	3.228	384	0.039	38.92	169	171	79.8	anisole-NHC-Pt→NHC-helicene (IL- & ML-CT)
3	3.410	364	0.005	30.28	169	172	54.3	anisole-NHC-Pt→NHC-helicene (IL- & ML-CT)
					168	171	22.1	NHC-helicene-Pt-dbm_{core}→NHC-helicene (π-π* & LL- & ML-CT)
4	3.434	361	0.032	57.57	168	170	75.8	NHC-helicene-Pt-dbm_{core}→dbm (π-π* & IL- & LL- & ML-CT)
5	3.573	347	0.466	82.31	168	171	29.4	NHC-helicene-Pt-dbm_{core}→NHC-helicene (π-π* & LL- & ML-CT)
					168	172	23.7	NHC-helicene-Pt-dbm_{core}→NHC-helicene (π-π* & LL- & ML-CT)
					169	172	19.7	anisole-NHC-Pt→NHC-helicene (IL- & ML-CT)
8	3.822	324	0.075	-26.60	167	170	64.9	anisole-NHC-helicene-Pt-dbm_{core}→dbm (π-π* & IL- & LL- & ML-CT)
9	3.840	323	0.085	-48.27	169	173	54.3	anisole-NHC-Pt→anisole-NHC-helicene-Pt (π-π* & MM & IL- & ML-CT)
10	3.924	316	0.094	-3.70	167	171	43.4	anisole-NHC-helicene-Pt-dbm_{core}→NHC-helicene (π-π* & IL- & LL- & ML-CT)
					167	172	18.3	anisole-NHC-helicene-Pt-dbm_{core}→NHC-helicene (π-π* & IL- & LL- & ML-CT)
					166	171	10.5	helicene-anisole-Pt→NHC-helicene (π-π* & IL- & ML-CT)
11	3.933	315	0.186	353.31	168	172	24.6	NHC-helicene-Pt-dbm_{core}→NHC-helicene

								(π-π* & LL- & ML-CT)
					167	171	26.2	anisole-NHC-helicene-Pt-dbm_{core}→NHC-helicene
								(π-π* & IL- & LL- & ML-CT)
					166	171	13.7	helicene-anisole-Pt→NHC-helicene
								(π-π* & IL- & ML-CT)
12	4.007	309	0.013	-53.43	165	171	35.9	Pt(d_{z2})→NHC-helicene
								(ML-CT)
					165	172	27.2	Pt(d_{z2})→NHC-helicene
								(ML-CT)
					165	173	24.1	Pt(d_{z2})→anisole-NHC-helicene-Pt
								(MM & ML-CT)
13	4.036	307	0.491	-108.61	164	170	79.6	anisole-Pt-dbm→dbm
								(π-π* & IL- & LL- & ML-CT)
14	4.161	298	0.171	18.57	166	170	70.6	helicene-anisole-Pt→dbm
								(LL- & ML-CT)
15	4.212	294	0.171	2.46	162	170	25.7	Pt-dbm→dbm
								(π-π* & IL- & ML-CT)
					167	172	25.5	anisole-NHC-helicene-Pt-dbm_{core}→NHC-helicene
								(π-π* & IL- & LL- & ML-CT)
					166	171	14.4	helicene-anisole-Pt→NHC-helicene
								(π-π* & IL- & ML-CT)
16	4.221	294	0.135	50.53	162	170	28.7	Pt-dbm→dbm
								(π-π* & IL- & ML-CT)
					167	172	21.4	anisole-NHC-helicene-Pt-dbm_{core}→NHC-helicene
								(π-π* & IL- & LL- & ML-CT)
19	4.302	288	0.297	-155.78	168	173	60.0	NHC-helicene-Pt-dbm_{core}→anisole-NHC-helicene-Pt
								(π-π* & MM & IL- & LL- & ML-CT)
					166	171	15.8	helicene-anisole-Pt→NHC-helicene
								(π-π* & IL- & ML-CT)

Table S2.6: *Selected dominant excitations and occupied (occ) – unoccupied (unocc) MO-pair contributions (greater than 10%) for helicene-NHC-Pt complex* ***Pt2-IV****. For MOs visualization, see Figure S2.7. Based on TDDFT-PBE0//SDD/SV(P) with continuum solvent model for toluene calculations.*

Excitation	*E* / eV	λ / nm	*f*	*R* / 10^{-40} cgs	occ no.	unocc no.	%	Assignment
1	3.157	393	0.075	-13.59	169	170	86.7	anisole-NHC-Pt→dbm (LL- & ML-CT)
2	3.228	384	0.039	42.42	169	171	79.8	anisole-NHC-Pt→NHC-helicene (IL- & ML-CT)
3	3.408	364	0.005	23.82	169	172	55.7	anisole-NHC-Pt→NHC-helicene (IL- & ML-CT)
					168	171	22.3	NHC-helicene-Pt-dbm_{core}→NHC-helicene (π-π* & LL- & ML-CT)
4	3.433	361	0.033	51.19	168	170	77.3	NHC-helicene-Pt-dbm_{core}→dbm (π-π* & IL- & LL- & ML-CT)
5	3.572	347	0.467	86.73	168	171	29.8	NHC-helicene-Pt-dbm_{core}→NHC-helicene (π-π* & LL- & ML-CT)
					168	172	23.8	NHC-helicene-Pt-dbm_{core}→NHC-helicene (π-π* & LL- & ML-CT)
					169	172	19.4	anisole-NHC-Pt→NHC-helicene (IL- & ML-CT)
8	3.819	325	0.091	-21.14	167	170	71.2	anisole-NHC-helicene-Pt-dbm_{core}→dbm (π-π* & IL- & LL- & ML-CT)
9	3.838	323	0.075	-51.68	169	173	57.2	anisole-NHC-Pt→anisole-NHC-helicene-Pt (π-π* & MM & IL- & ML-CT)
10	3.923	316	0.091	-24.27	167	171	39.0	anisole-NHC-helicene-Pt-dbm_{core}→NHC-helicene (π-π* & IL- & LL- & ML-CT)
					167	172	19.7	anisole-NHC-helicene-Pt-dbm_{core}→NHC-helicene (π-π* & IL- & LL- & ML-CT)
					166	171	12.0	helicene-anisole-Pt→NHC-helicene

								(π-π* & IL- & ML-CT)
11	3.932	315	0.192	349.81	167	171	31.1	anisole-NHC-helicene-Pt-dbm_{core}→NHC-helicene (π-π* & IL- & LL- & ML-CT)
					168	172	24.1	NHC-helicene-Pt-dbm_{core}→NHC-helicene (π-π* & LL- & ML-CT)
					166	171	13.0	helicene-anisole-Pt→NHC-helicene (π-π* & IL- & ML-CT)
12	4.006	309	0.013	-42.35	165	171	36.9	Pt(d_{z2})→NHC-helicene (ML-CT)
					165	172	29.8	Pt(d_{z2})→NHC-helicene (ML-CT)
					165	173	25.0	Pt(d_{z2})→anisole-NHC-helicene-Pt (MM & ML-CT)
13	4.038	307	0.475	-102.26	164	170	80.8	anisole-Pt-dbm→dbm (π-π* & IL- & LL- & ML-CT)
14	4.164	298	0.172	2.96	166	170	71.1	helicene-anisole-Pt→dbm (LL- & ML-CT)
15	4.210	294	0.110	12.49	162	170	39.0	Pt-dbm→dbm (π-π* & IL- & ML-CT)
					167	172	18.5	anisole-NHC-helicene-Pt-dbm_{core}→NHC-helicene (π-π* & IL- & LL- & ML-CT)
16	4.219	294	0.206	14.17	167	172	27.0	anisole-NHC-helicene-Pt-dbm_{core}→NHC-helicene (π-π* & IL- & LL- & ML-CT)
					162	170	21.9	Pt-dbm→dbm (π-π* & IL- & ML-CT)
19	4.299	288	0.287	-170.27	168	173	62.4	NHC-helicene-Pt-dbm_{core}→anisole-NHC-helicene-Pt (π-π* & MM & IL- & LL- & ML-CT)
					166	171	17.0	helicene-anisole-Pt→NHC-helicene (π-π* & IL- & ML-CT)

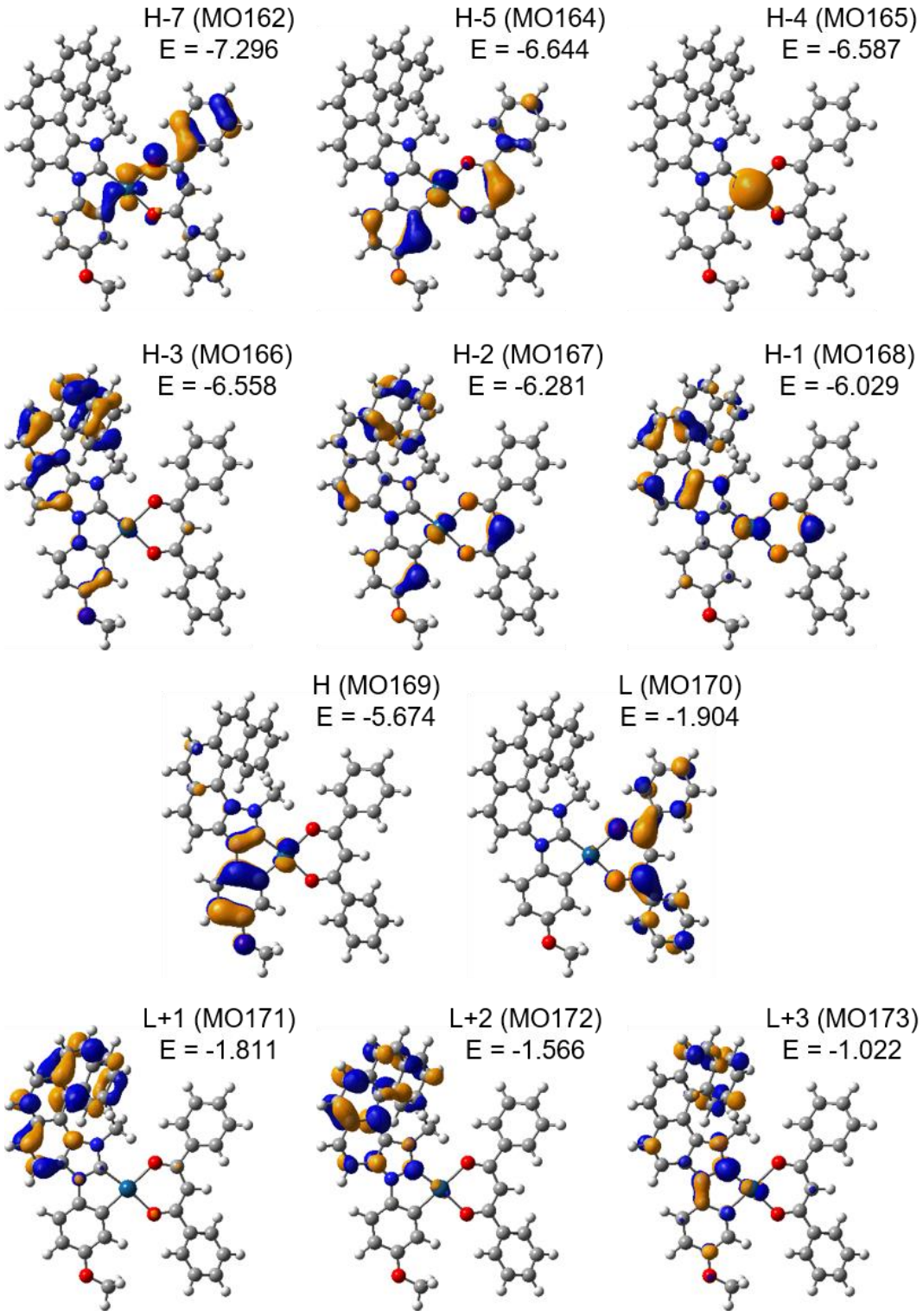

Figure S2.7: *Isosurfaces (±0.04 au) of MOs involved in selected electronic transitions of* ***Pt2-I****. Based on PBE0//SDD/SV(P) with continuum solvent model for toluene calculations. H = HOMO, L = LUMO. Values E listed are orbital energies, in eV. Isosurfaces of the corresponding MOs for* ***Pt2*** *conformers II-IV appeared to be very similar and therefore they are not shown.*

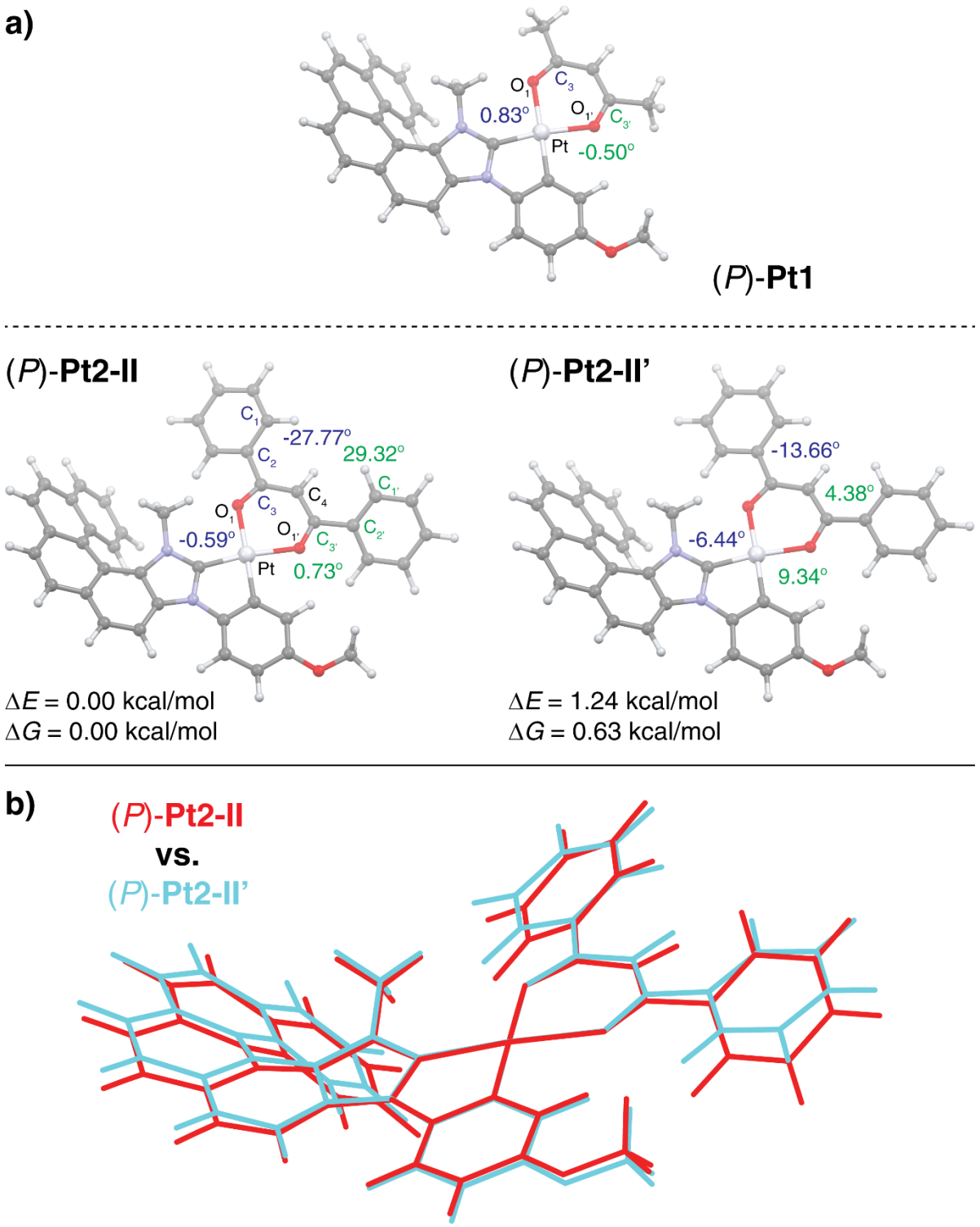

Figure S2.8: *a) Selected optimized (TDA-TDDFT-PBE0//SDD/SV(P) with continuum solvent model for toluene) triplet excited-state structures of helicene-NHC-Pt complexes* ***Pt1*** *and* ***Pt2****. Values listed are dihedral angles (as defined on the structures* ***Pt1*** *and* ***Pt2-II****) and relative energies ΔE and free energies ΔG. b) Overlay of the corresponding* ***Pt2-II*** *(red) and* ***Pt2-II'*** *(blue) structures. See Table S2.7 for a full set of computed results.*

Table S2.7: *Structural, energetic and electronic characterization of optimized triplet excited-state structures of helicene-NHC-Pt complexes* ***Pt1*** *and* ***Pt2****: ∠ – dihedral angles as defined in Figure S2.8, in degree; ΔE and ΔG – relative energy and free-energy values, in kcal/mol; λ – T_1-S_0 energy difference at optimized T_1 excited-state geometry, corresponding to phosphorescence energy, in nm; assignment – MO-to-MO: % transitions assignment (for MO-pair contributions greater than 10%), see Figures S2.9-S2.11 for MOs isosurfaces (see also Figure S2.12). Based on TDDFT- and TDA-TDDFT-PBE0//SDD/SV(P) with continuum solvent model for toluene calculations.*

Structure	∠$C_1C_2C_3C_4$	∠$C_{1'}C_{2'}C_{3'}C_4$	∠$C_3O_1PtO_{1'}$	∠$C_{3'}O_{1'}PtO_1$	Δ*E*	Δ*G*	λ	assignment
TDA-TDDFT-PBE0//SDD/SV(P) PCM(toluene)								
Pt1	–	–	0.83	-0.50	–	–	568	138-to-136: 53.5 NHC-helicene→anisole-NHC-helicene-Pt-acac (π-π* & IL- & LL- & LM-CT) 138-to-137: 28.2 NHC-helicene→ anisole-NHC-helicene-Pt (π-π* & IL- & LM-CT)
Pt2-I	-27.70	-28.39	-0.95	-0.68	0.00	0.35	568	170-to-168: 52.5 NHC-helicene→anisole-NHC-helicene-Pt-acac (π-π* & IL- & LL- & LM-CT) 170-to-169: 29.4 NHC-helicene→ anisole-NHC-helicene-Pt (π-π* & IL- & LM-CT)
Pt2-II	-27.77	29.32	-0.59	0.73	0.00	0.00	569	170-to-168: 52.2 NHC-helicene→anisole-NHC-helicene-Pt-acac (π-π* & IL- & LL- & LM-CT) 170-to-169: 29.9 NHC-helicene→ anisole-NHC-helicene-Pt (π-π* & IL- & LM-CT)
Pt2-II'	-13.66	4.38	-6.44	9.34	1.24	0.63	535	170-to-168: 60.8 dbm-Pt→NHC-helicene-Pt-dbm_{core} (π-π* & MM & IL- & LL- & LM-CT) 170-to-167: 19.7 dbm-Pt→ anisole-NHC-helicene-Pt-dbm_{core}

								(π-π* & MM & IL- & LL- & LM-CT)
Pt2-II''	-13.27	11.09	-19.78	23.27	1.22	2.39	544	170-to-168: 61.3 dbm-Pt→NHC-helicene-Pt-dbm_{core} (π-π* & MM & IL- & LL- & LM-CT) 170-to-167: 20.5 dbm-Pt→ anisole-NHC-helicene-Pt-dbm_{core} (π-π* & MM & IL- & LL- & LM-CT)
Pt2-III	27.80	29.24	3.36	0.83	0.57	0.51	565	170-to-168: 53.8 NHC-helicene→anisole-NHC-helicene-Pt-acac (π-π* & IL- & LL- & LM-CT) 170-to-169: 27.9 NHC-helicene→ anisole-NHC-helicene-Pt (π-π* & IL- & LM-CT)
Pt2-IV	27.58	-28.09	3.12	-0.72	0.60	0.66	565	170-to-168: 54.1 NHC-helicene→anisole-NHC-helicene-Pt-acac (π-π* & IL- & LL- & LM-CT) 170-to-169: 27.4 NHC-helicene→ anisole-NHC-helicene-Pt (π-π* & IL- & LM-CT)
				TDDFT-PBE0//SDD/SV(P) PCM(toluene)				
Pt1	–	–	0.86	-0.53	–	–	685	138-to-136: 65.4 NHC-helicene→NHC-helicene-Pt-acac (π-π* & LL- & LM-CT) 138-to-135: 11.2 NHC-helicene→ anisole-NHC-helicene-Pt-acac (π-π* & IL- & LL- & LM-CT)
Pt2-II	-27.98	29.22	-0.82	0.83	–	–	684	170-to-168: 59.0 NHC-helicene→anisole-NHC-helicene-Pt-acac (π-π* & IL- & LL- & LM-CT) 170-to-169: 12.6

Pt2-II'	-13.91	2.64	-4.78	7.37	–	–	565	NHC-helicene→ anisole-NHC-helicene-Pt (π-π* & IL- & LM-CT) 170-to-168: 59.5 dbm-Pt→NHC-helicene-Pt-dbm_{core} (π-π* & MM & IL- & LL- & LM-CT) 170-to-167: 21.0 dbm-Pt→ anisole-NHC-helicene-Pt-dbm_{core} (π-π* & MM & IL- & LL- & LM-CT)

Table S2.8: *Structural, energetic and electronic characterization of optimized triplet excited-state structures of helicene-NHC-Pt complexes **Pt1** and **Pt2**: ∠ – dihedral angles as defined in Figure S2.8, in degree; ΔE and ΔG – relative energy and free-energy values, in kcal/mol; λ – T_1-S_0 energy difference at optimized T_1 excited-state geometry, corresponding to phosphorescence energy, in nm; assignment – MO-to-MO: % transitions assignment (for MO-pair contributions greater than 10%), see Figures S2.9-S2.11 for MOs isosurfaces (see also Figure S2.12). Based on TDDFT- and TDA-TDDFT-PBE0//SDD/SV(P) with continuum solvent model for THF calculations.*

Structure	$\angle C_1C_2C_3C_4$	$\angle C_{1'}C_{2'}C_{3'}C_4$	$\angle C_3O_1PtO_{1'}$	$\angle C_{3'}O_{1'}PtO_1$	ΔE	ΔG	λ	assignment
TDA-TDDFT-PBE0//SDD/SV(P) PCM(THF)								
Pt1	–	–	0.42	-0.12	–	–	565	138-to-136: 45.8 NHC-helicene→anisole-NHC-helicene-Pt-acac (π-π* & IL- & LL- & LM-CT)
Pt2-I	-26.98	-27.53	-1.89	0.06	0.04	0.14	566	138-to-137: 38.3 NHC-helicene→ anisole-NHC-helicene-Pt (π-π* & IL- & LM-CT) 170-to-168: 43.3 NHC-helicene→anisole-NHC-helicene-Pt-acac (π-π* & IL- & LL- & LM-CT) 170-to-169: 39.1 NHC-helicene→ anisole-NHC-helicene-Pt (π-π* & IL- & LM-CT)
Pt2-II	-27.16	28.12	-0.75	1.27	0.00	0.00	566	170-to-168: 43.6 NHC-helicene→anisole-NHC-helicene-Pt-acac

								(π-π* & IL- & LL- & LM-CT)
								170-to-169: 40.0
								NHC-helicene→ anisole-NHC-helicene-Pt
								(π-π* & IL- & LM-CT)
								170-to-168: 49.9
Pt2-II''	-11.62	10.42	-22.57	26.69	1.21	2.38	543	dbm-Pt→NHC-helicene-Pt-dbm_{core}
								(π-π* & MM & IL- & LL- & LM-CT)
								170-to-167: 34.2
								dbm-Pt→ anisole-NHC-helicene-Pt-dbm_{core}
								(π-π* & MM & IL- & LL- & LM-CT)
								170-to-168: 43.6
Pt2-III	27.24	28.48	2.62	1.54	0.49	0.78	564	NHC-helicene→anisole-NHC-helicene-Pt-acac
								(π-π* & IL- & LL- & LM-CT)
								170-to-169: 36.2
								NHC-helicene→ anisole-NHC-helicene-Pt
								(π-π* & IL- & LM-CT)
								170-to-168: 43.8
Pt2-IV	27.22	-27.38	1.67	0.48	0.49	0.70	563	NHC-helicene→anisole-NHC-helicene-Pt-acac
								(π-π* & IL- & LL- & LM-CT)
								170-to-169: 35.6
								NHC-helicene→ anisole-NHC-helicene-Pt
								(π-π* & IL- & LM-CT)
TDDFT-PBE0//SDD/SV(P) PCM(THF)								
								138-to-136: 67.7
Pt1	–	–	0.50	-0.20	–	–	686	NHC-helicene→NHC-helicene-Pt-acac
								(π-π* & LL- & LM-CT)
								170-to-168: 64.4
Pt2-II	-27.71	28.10	-1.08	1.53	–	–	685	NHC-helicene→anisole-NHC-helicene-Pt-acac
								(π-π* & IL- & LL- & LM-CT)
								170-to-168: 48.0
Pt2-II''	-11.94	8.77	-19.23	23.17	–	–	569	dbm-Pt→NHC-helicene-Pt-dbm_{core}

			(π-π* & MM & IL- & LL- & LM-CT) 170-to-167: 35.2 dbm-Pt⟶ anisole-NHC-helicene-Pt-dbm_{core} (π-π* & MM & IL- & LL- & LM-CT)

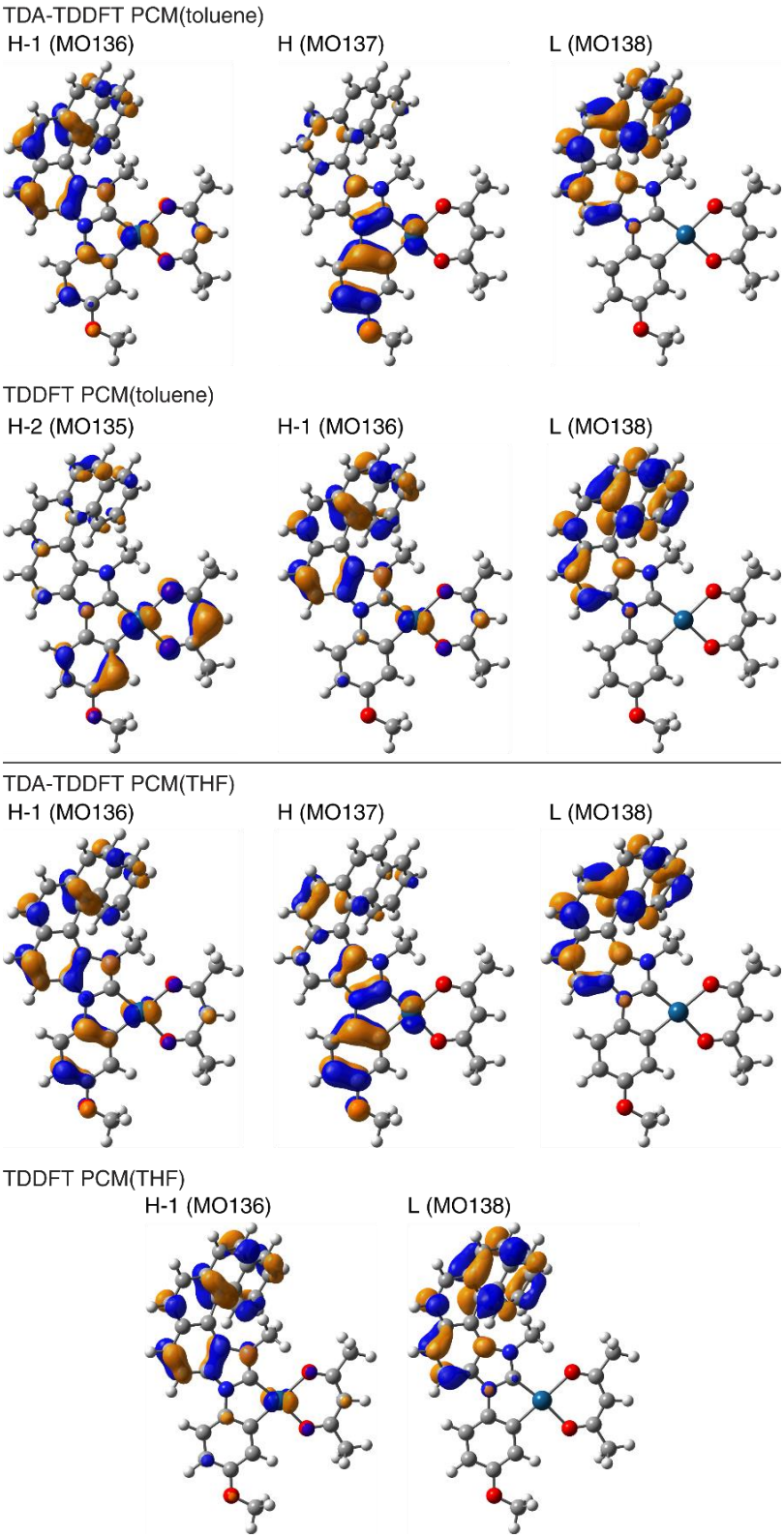

Figure S2.9: *Isosurfaces (±0.04 au) of MOs of S_0 at T_1 excited-state geometry (optimized at TDDFT- or TDA-TDDFT-PBE0//SDD/SV(P) PCM(toluene) or PCM(THF) level, as indicated) involved in T_1-S_0 emission transitions of* ***Pt1****. H = HOMO, L = LUMO.*

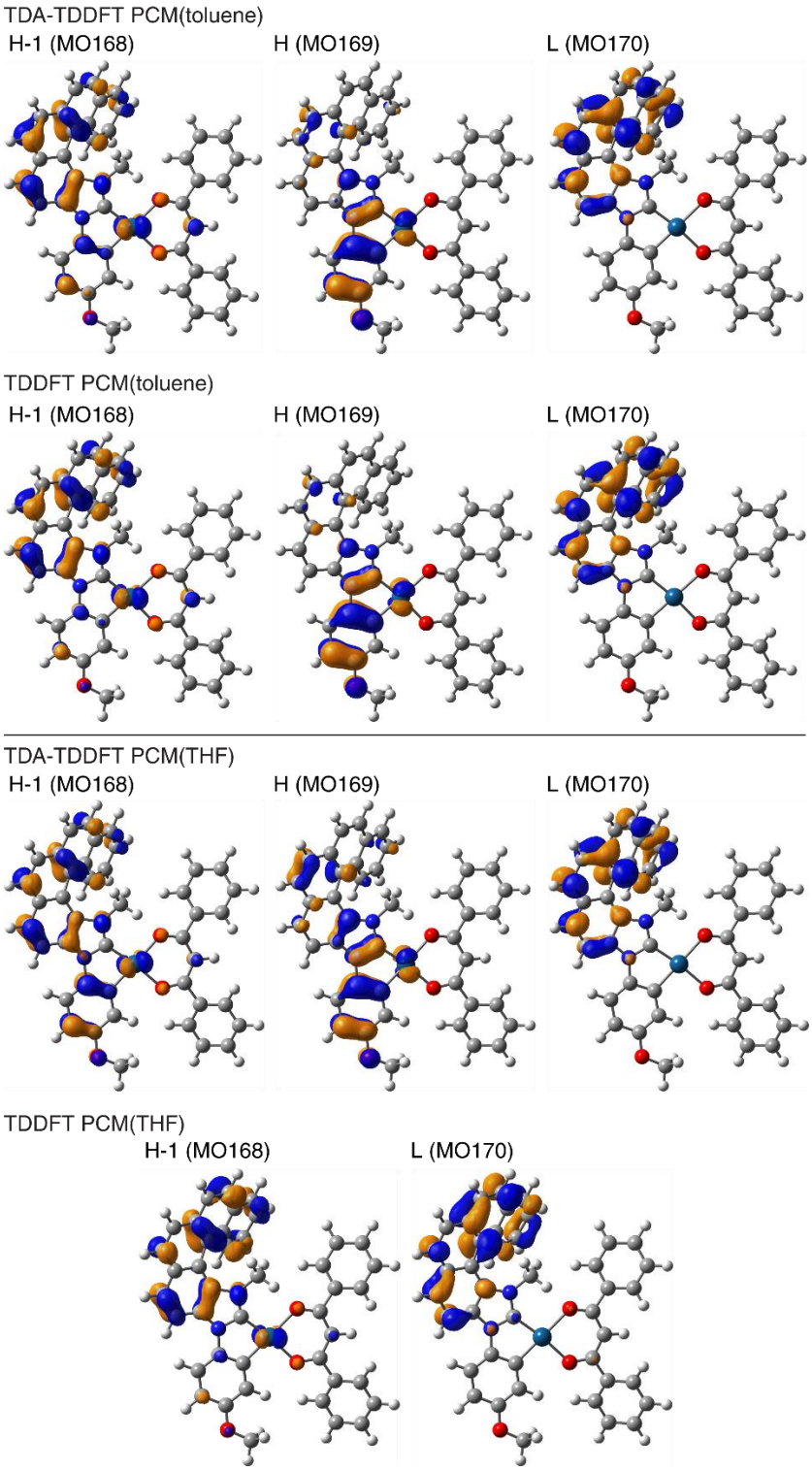

Figure S2.10: *Isosurfaces (±0.04 au) of MOs of S_0 at T_1 excited-state geometry (optimized at TDDFT- or TDA-TDDFT-PBE0//SDD/SV(P) PCM(toluene) or PCM(THF) level, as indicated) involved in T_1-S_0 emission transitions of* ***Pt2-II****. H = HOMO, L = LUMO. Isosurfaces of the corresponding MOs for other computed T_1 rotameric structures,* ***Pt2-I****,* ***Pt2-III*** *and* ***Pt2-IV****, appeared to be very similar and therefore they are not shown.*

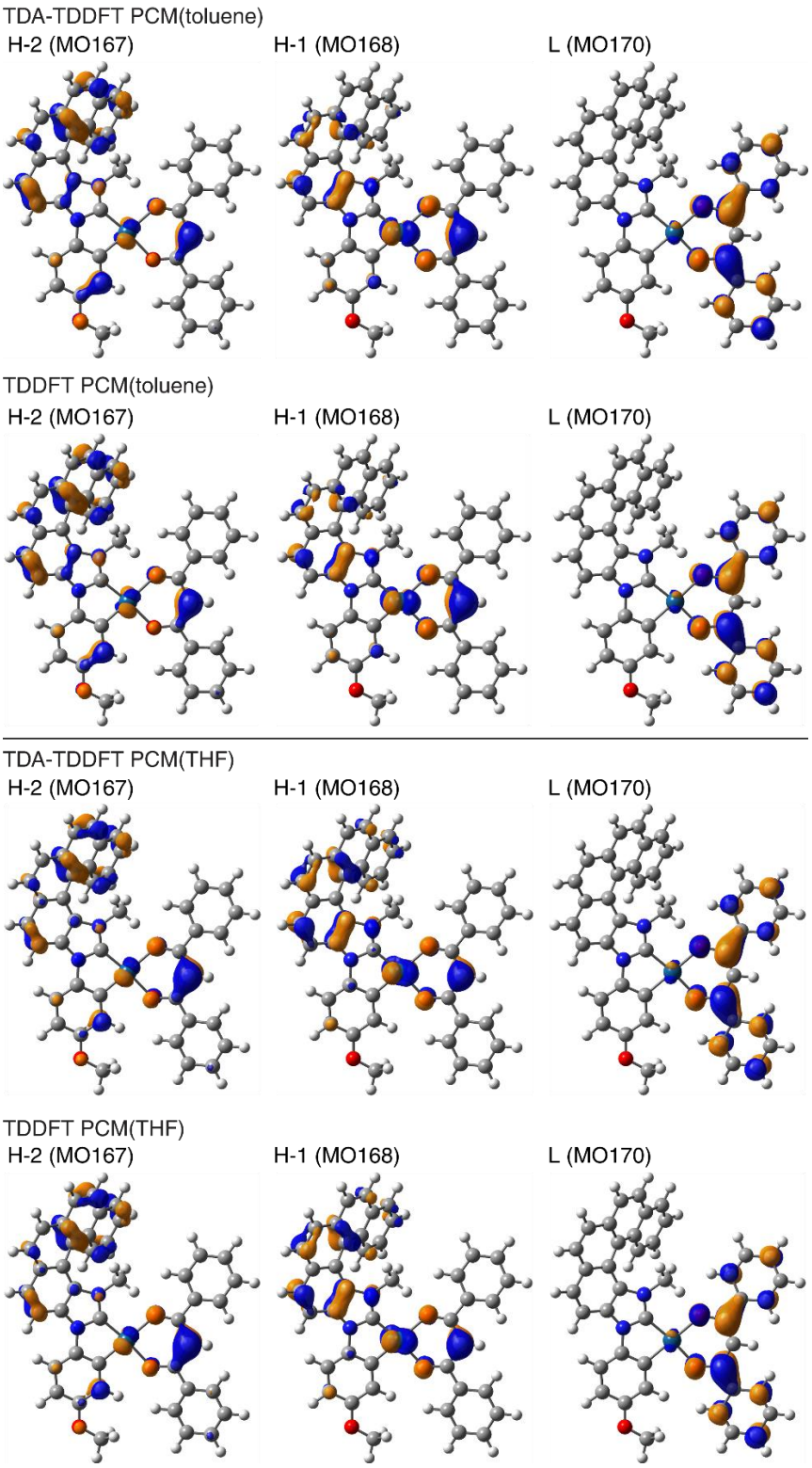

Figure S2.11: *Isosurfaces (±0.04 au) of MOs of S_0 at T_1 excited-state geometry (optimized at TDDFT- or TDA-TDDFT-PBE0//SDD/SV(P) PCM(toluene) or PCM(THF) level, as indicated) involved in T_1-S_0 emission transitions of* ***Pt2-II'*** *(for PCM(toluene)) and* ***Pt2-II"*** *(for PCM(THF); isosurfaces representative also for* ***Pt2-II"*** *for PCM(toluene)). H = HOMO, L = LUMO.*

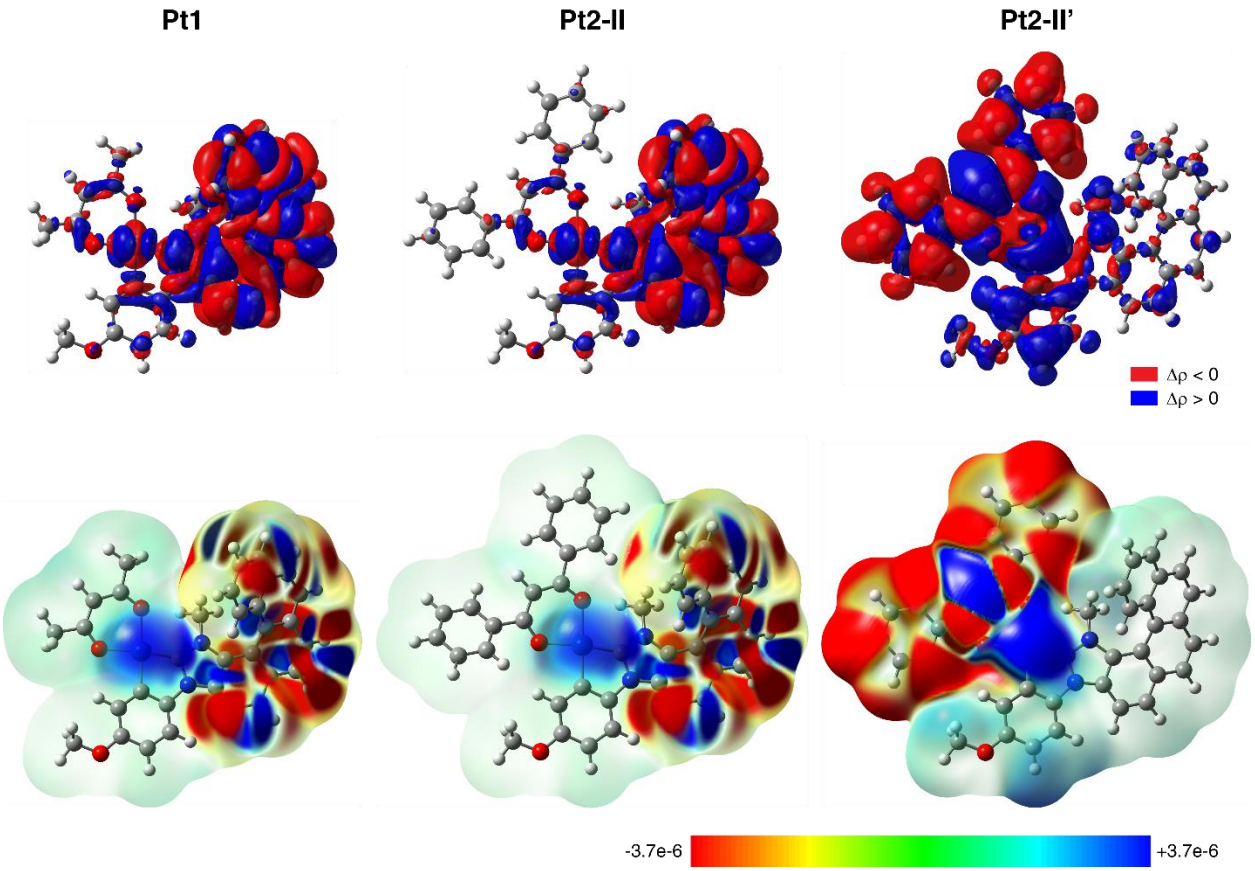

Figure S2.12: *Isosurfaces (±0.0001 au) of the electron difference density between the S_0 ground state and T_1 excited state, $\Delta\rho = \rho_g - \rho_e$ (top) along with isosurfaces (0.0001 au) of ρ_g color-mapped using the value of $\Delta\rho$ (bottom) for the helicene-NHC-Pt complexes **Pt1** and **Pt2** (conformers II and II') based on the TDA-TDDFT-PBE0//SDD/SV(P) PCM(toluene) calculations. Electron density moves from the red region to the blue region when moving from the excited state to the ground state. Note that TDA-TDDFT-PBE0//SDD/SV(P) PCM(THF) and the corresponding TDDFT-PBE0//SDD/SV(P) PCM(toluene) and PCM(THF) calculations gave essentially the same results.*

S2.3. Cartesian coordinates for optimized structures

Optimized (DFT-B3LYP//SDD/SV(P) with continuum solvent (toluene) model) geometries of the studied systems along with the corresponding absolute energies:

The atomic symbol followed by three Cartesian coordinates, in Å.

(*P*)-**Pt1**

Total energy = -1688.549796 au

C	2.525393	1.245967	0.135346
C	1.545090	2.254076	0.265208
C	1.884676	3.571892	0.579913
C	3.230183	3.909275	0.737992
C	4.227846	2.931095	0.591939
C	3.870489	1.601653	0.298474

N	0.225560	1.749850	0.073700
C	0.140106	0.403634	-0.162204
N	-1.175789	0.108626	-0.335757
C	-1.947520	1.272477	-0.183664
C	-1.034057	2.329872	-0.006768
C	-3.354100	1.504057	-0.266709
C	-3.718658	2.869885	-0.531450
C	-2.764916	3.918486	-0.397878
C	-1.444199	3.677478	-0.078199
C	-4.418238	0.523089	-0.129196
C	-5.675221	0.825288	-0.720487
C	-5.954616	2.154403	-1.170407
C	-5.044829	3.158530	-0.982873
C	-4.324187	-0.685266	0.677288
C	-5.358848	-1.673949	0.580865
C	-6.510581	-1.413543	-0.229010
C	-6.687354	-0.186117	-0.803023
C	-3.320742	-0.885180	1.664467
C	-3.282893	-2.031276	2.440724
C	-4.247621	-3.047306	2.264653
C	-5.272096	-2.860518	1.355010
C	-1.625865	-1.148857	-0.934250
Pt	1.824690	-0.599870	-0.212233
O	1.052554	-2.573711	-0.538837
C	1.734093	-3.643708	-0.628503
C	0.920121	-4.904061	-0.845755
O	5.508959	3.357724	0.759472
C	6.567095	2.433618	0.634128
O	3.739150	-1.451209	-0.205411
C	4.041425	-2.683117	-0.347487
C	5.526088	-2.975935	-0.289171
C	3.139308	-3.744747	-0.545838
H	-0.741522	4.501911	0.030154
H	-3.101443	4.946582	-0.559607
H	-5.299209	4.194851	-1.225016
H	-6.940241	2.366854	-1.595356
H	-7.614227	0.050955	-1.334583
H	-7.281549	-2.185661	-0.313478
H	-6.057728	-3.614840	1.244198
H	-4.202245	-3.959167	2.867678
H	-2.502691	-2.143140	3.199727
H	-2.574140	-0.109371	1.839150
H	1.127708	4.343630	0.721969
H	3.526924	4.932332	0.981568
H	4.628251	0.823223	0.199003
H	6.496150	1.623459	1.385525
H	7.495647	3.000845	0.804396
H	6.600043	1.981759	-0.376168
H	-0.831059	-1.519890	-1.593480
H	-2.538164	-0.955832	-1.515565
H	-1.832942	-1.909648	-0.169450
H	3.568857	-4.742850	-0.645898
H	5.754032	-4.046188	-0.411075
H	6.044093	-2.404170	-1.080503
H	5.930971	-2.628099	0.678529
H	1.543731	-5.809103	-0.913035
H	0.199691	-5.023038	-0.016191
H	0.329321	-4.804473	-1.774539

(*P*)-**Pt2-I**

Total energy = -2071.746065 au

C	-3.121814	2.417788	-0.227379
C	-1.724771	2.617407	-0.290979
C	-1.193140	4.016235	-0.420930
C	0.091594	4.303438	0.076538
C	0.627073	5.588686	-0.025122
C	-0.106013	6.608729	-0.642918
C	-1.378486	6.332818	-1.154854
C	-1.920091	5.049547	-1.040346
H	-2.906606	4.848623	-1.465478
H	-1.953136	7.120505	-1.651930
H	0.314994	7.615365	-0.729128
H	1.623408	5.795109	0.378200
H	0.662751	3.503603	0.552726
H	-3.748025	3.305933	-0.273377
C	-3.786082	1.180671	-0.112133
C	-5.285586	1.157530	-0.062266
C	-6.040501	2.218819	0.469756
H	-5.537103	3.094309	0.887626
C	-7.436003	2.152664	0.505692
H	-8.006488	2.981738	0.935691
C	-8.101066	1.030401	0.000190
H	-9.194258	0.982185	0.023465
C	-7.360280	-0.031896	-0.531172
H	-7.873667	-0.912147	-0.930718
C	-5.965493	0.027310	-0.553152
H	-5.383239	-0.800413	-0.964722
O	-3.229521	0.030804	-0.066757
O	-0.839289	1.703276	-0.230243
Pt	-1.183397	-0.409769	-0.092200
C	-1.494388	-2.379823	0.110555
C	-2.737806	-3.007180	0.260828
H	-3.637570	-2.391590	0.228102
C	-2.816987	-4.397550	0.465393
O	-3.983465	-5.080908	0.617072
C	-5.205685	-4.377332	0.590370
H	-5.998262	-5.127626	0.737884
H	-5.365934	-3.869570	-0.380606
H	-5.264704	-3.624827	1.400199
C	-1.641741	-5.164091	0.534087
H	-1.723389	-6.239476	0.709783
C	-0.394168	-4.554274	0.390695
H	0.504462	-5.165719	0.476923
C	-0.330705	-3.177186	0.165459
N	0.857671	-2.406338	0.009920
C	0.670173	-1.055782	-0.115441
N	1.898081	-0.493110	-0.275256
C	2.081536	0.869015	-0.776701
H	2.941382	0.880137	-1.462291
H	2.260641	1.580567	0.040625
H	1.169371	1.165430	-1.308737
C	2.886890	-1.489965	-0.227036
C	2.204073	-2.717595	-0.130145
C	2.867924	-3.947390	-0.320761
H	2.343325	-4.900242	-0.275657
C	4.200466	-3.895796	-0.676075

H 4.727023 -4.820537 -0.929021
C 4.925670 -2.671890 -0.733167
C 6.267984 -2.654419 -1.226978
H 6.713577 -3.596874 -1.559392
C 6.955740 -1.477685 -1.343669
H 7.949738 -1.455350 -1.800449
C 6.434511 -0.270609 -0.779444
C 7.223381 0.925802 -0.792669
H 8.160935 0.921649 -1.357284
C 6.826144 2.043750 -0.114427
H 7.425784 2.958682 -0.146384
C 5.673572 2.003028 0.734111
C 5.379395 3.082208 1.608125
H 5.995373 3.985227 1.548258
C 4.370758 2.985638 2.549164
H 4.167093 3.817849 3.229724
C 3.633984 1.785324 2.655623
H 2.875052 1.676699 3.436324
C 3.871570 0.736532 1.783216
H 3.300168 -0.184996 1.903128
C 4.859317 0.822692 0.764005
C 5.162410 -0.272925 -0.144894
C 4.308338 -1.431233 -0.348667

(*P*)-**Pt2-II**

Total energy = -2071.746040 au

C -3.118460 2.417380 -0.227583
C -1.721475 2.614907 -0.304612
C -1.188274 4.014829 -0.412947
C 0.102653 4.291370 0.074097
C 0.638204 5.577869 -0.009800
C -0.101603 6.610160 -0.598580
C -1.380795 6.345327 -1.099541
C -1.921832 5.060403 -1.003075
H -2.914082 4.867651 -1.418394
H -1.961034 7.143144 -1.573407
H 0.319261 7.617974 -0.670539
H 1.639606 5.775790 0.385131
H 0.678536 3.482366 0.528523
H -3.739276 3.310094 -0.190420
C -3.782945 1.180830 -0.105538
C -5.279397 1.163044 0.001184
C -6.089446 2.142924 -0.600931
H -5.634130 2.944398 -1.188145
C -7.481179 2.084774 -0.488139
H -8.096530 2.848057 -0.974410
C -8.085951 1.053141 0.237983
H -9.175726 1.011548 0.330631
C -7.289859 0.072518 0.841552
H -7.755934 -0.735824 1.413720
C -5.900179 0.121927 0.716023
H -5.274988 -0.642148 1.184029
O -3.226932 0.031231 -0.049523
O -0.837621 1.698025 -0.267213
Pt -1.182632 -0.414222 -0.118931
C -1.494491 -2.386984 0.054455
C -2.740076 -3.020914 0.149934
H -3.640655 -2.408689 0.088242

C	-2.820994	-4.415256	0.324958
O	-3.989184	-5.105985	0.419742
C	-5.213249	-4.412416	0.320149
H	-6.007049	-5.170465	0.410277
H	-5.314982	-3.895848	-0.653671
H	-5.331320	-3.668907	1.132302
C	-1.645896	-5.178931	0.421340
H	-1.729397	-6.257623	0.574422
C	-0.396523	-4.563717	0.324459
H	0.500783	-5.175114	0.422804
C	-0.330527	-3.182997	0.123637
N	0.859351	-2.409625	-0.007688
C	0.670819	-1.059816	-0.140195
N	1.899367	-0.494989	-0.286354
C	2.086288	0.865119	-0.791893
H	2.949464	0.872979	-1.473462
H	2.262355	1.579409	0.023650
H	1.176837	1.160371	-1.329126
C	2.889592	-1.489420	-0.221825
C	2.208384	-2.718306	-0.128908
C	2.878379	-3.947013	-0.304793
H	2.356825	-4.901468	-0.260368
C	4.215079	-3.893325	-0.643908
H	4.747292	-4.817860	-0.885518
C	4.937549	-2.667744	-0.698187
C	6.285483	-2.648457	-1.176416
H	6.737566	-3.590963	-1.499798
C	6.971148	-1.470193	-1.289990
H	7.970281	-1.446778	-1.735366
C	6.440027	-0.262398	-0.736573
C	7.225696	0.936146	-0.745056
H	8.169708	0.932587	-1.298812
C	6.817645	2.055382	-0.075378
H	7.415102	2.971863	-0.103733
C	5.655514	2.014450	0.759996
C	5.348422	3.095773	1.626924
H	5.962776	4.000163	1.571262
C	4.329171	2.999712	2.556515
H	4.115520	3.833603	3.231932
C	3.594237	1.797841	2.658434
H	2.826525	1.689915	3.430599
C	3.844702	0.746741	1.792455
H	3.274246	-0.175846	1.908733
C	4.844076	0.832053	0.784531
C	5.160634	-0.265882	-0.116875
C	4.312213	-1.427342	-0.326255

(*P*)-**Pt2-III**

Total energy = -2071.745461 au

C	-1.860791	5.101736	0.211808
C	-1.186060	4.013158	-0.371042
C	0.033790	4.254370	-1.029191
C	0.554363	5.546548	-1.120848
C	-0.126816	6.621591	-0.538142
C	-1.332623	6.393291	0.133485
C	-1.711198	2.607375	-0.297287
C	-3.108335	2.408365	-0.224984
C	-3.775278	1.171422	-0.130876

C	-5.274414	1.152568	-0.072208
C	-5.916906	0.108410	0.618570
C	-7.309818	0.057588	0.699873
C	-8.087131	1.039771	0.074778
C	-7.460303	2.074215	-0.628278
C	-6.065694	2.133992	-0.696591
O	-3.219564	0.022256	-0.063483
Pt	-1.175789	-0.422737	-0.142921
C	-1.489121	-2.391889	0.070003
C	-0.325850	-3.187449	0.157302
C	-0.393686	-4.564589	0.380571
C	-1.643770	-5.177043	0.485028
C	-2.817893	-4.414097	0.373469
C	-2.735339	-3.023095	0.174075
N	0.864733	-2.417020	0.015800
C	0.675528	-1.071242	-0.149703
N	1.903809	-0.508012	-0.297071
C	2.896157	-1.496976	-0.195729
C	2.216150	-2.724918	-0.079294
C	4.320774	-1.433634	-0.274747
C	4.955223	-2.683432	-0.597300
C	4.234330	-3.908851	-0.522234
C	2.891657	-3.956398	-0.207549
C	5.163464	-0.264270	-0.083281
C	6.456633	-0.278933	-0.673797
C	7.000959	-1.502072	-1.178213
C	6.313215	-2.676969	-1.046042
C	4.823865	0.864612	0.771253
C	5.636054	2.046048	0.726491
C	6.819046	2.059287	-0.080115
C	7.242755	0.919132	-0.702702
C	3.797160	0.815727	1.753430
C	3.523592	1.897591	2.573371
C	4.262012	3.094672	2.449332
C	5.306977	3.157185	1.546075
C	2.084026	0.840101	-0.836115
O	-3.986834	-5.102150	0.478038
C	-5.210193	-4.408762	0.369784
O	-0.827747	1.690055	-0.327594
H	2.371756	-4.910627	-0.143963
H	4.773509	-4.838483	-0.725805
H	6.772660	-3.628199	-1.331220
H	8.010129	-1.490750	-1.600830
H	8.199556	0.897851	-1.233659
H	7.417352	2.974625	-0.123964
H	5.923015	4.059339	1.474608
H	4.028313	3.953128	3.086067
H	2.733084	1.818137	3.325675
H	3.223726	-0.102166	1.888986
H	0.502631	-5.175411	0.490015
H	-1.728514	-6.252958	0.655894
H	-3.635211	-2.411404	0.099302
H	-5.326403	-3.653901	1.171737
H	-6.004727	-5.164583	0.471466
H	-5.312565	-3.905901	-0.611114
H	1.255476	1.045484	-1.526506
H	3.038571	0.878836	-1.378128
H	2.080807	1.598250	-0.041438

H	-3.732389	3.299163	-0.241059
H	-5.306364	-0.657266	1.102867
H	-7.793155	-0.753298	1.253846
H	-9.179275	0.997050	0.132489
H	-8.060403	2.838520	-1.131715
H	-5.593025	2.937601	-1.267033
H	0.564842	3.413671	-1.479663
H	1.498040	5.716311	-1.648644
H	0.283127	7.634296	-0.603992
H	-1.865285	7.225406	0.604239
H	-2.793423	4.939909	0.758058

(*P*)-**Pt2-IV**

Total energy = -2071.745446 au

Pt	-1.173492	-0.418926	-0.119723
O	-3.976172	-5.076695	0.661974
O	-3.219519	0.016117	-0.079547
O	-0.832702	1.696406	-0.294126
N	0.868254	-2.412423	0.034508
N	1.906018	-0.504487	-0.287681
C	0.678640	-1.066301	-0.127407
C	2.218054	-2.721822	-0.075210
C	2.898320	-1.494653	-0.197678
C	2.890043	-3.954253	-0.211954
H	2.368655	-4.907522	-0.145108
C	4.229676	-3.908379	-0.539508
H	4.765476	-4.838532	-0.749515
C	4.951651	-2.683890	-0.620017
C	4.322200	-1.433268	-0.290675
C	6.305460	-2.679271	-1.081210
H	6.760838	-3.631076	-1.370948
C	6.993785	-1.505388	-1.219187
H	7.999071	-1.495472	-1.650989
C	6.455944	-0.281590	-0.709488
C	5.168402	-0.265202	-0.106828
C	7.243404	0.915403	-0.745783
H	8.195158	0.892804	-1.285682
C	6.827053	2.056185	-0.119411
H	7.426087	2.970751	-0.169026
C	5.651715	2.044543	0.698340
C	4.838532	0.864106	0.751002
C	5.331815	3.156207	1.520828
H	5.948235	4.057601	1.443326
C	4.295469	3.095077	2.434070
H	4.068924	3.953922	3.072871
C	3.556957	1.898844	2.565478
H	2.773704	1.820368	3.325433
C	3.821368	0.816526	1.743111
H	3.248317	-0.100730	1.884448
C	-0.320554	-3.181023	0.198101
C	-0.385679	-4.554154	0.445768
H	0.512008	-5.164747	0.545598
C	-1.634086	-5.161394	0.592780
H	-1.716728	-6.233719	0.785823
C	-2.808814	-4.396152	0.504814
C	-2.728316	-3.009564	0.276449
H	-3.627678	-2.394443	0.228442
C	-1.484121	-2.385046	0.121576

C	-5.198322	-4.374095	0.613649
H	-5.263263	-3.606732	1.408935
H	-5.991756	-5.121797	0.769463
H	-5.351767	-3.884473	-0.367689
C	2.081601	0.843800	-0.827638
H	1.247307	1.049187	-1.511184
H	3.031456	0.883042	-1.377751
H	2.085121	1.601598	-0.032616
C	-3.780750	1.163348	-0.133079
C	-3.118821	2.403491	-0.221922
H	-3.747409	3.286230	-0.318007
C	-1.721609	2.608878	-0.285047
C	-5.280878	1.131690	-0.125005
C	-5.940799	-0.002917	-0.632732
H	-5.342876	-0.827774	-1.027244
C	-7.335331	-0.069849	-0.649141
H	-7.832617	-0.953519	-1.061290
C	-8.096366	0.989316	-0.140680
H	-9.189503	0.935213	-0.147768
C	-7.451738	2.116308	0.380539
H	-8.038506	2.943381	0.792069
C	-6.056215	2.189716	0.383427
H	-5.569179	3.069065	0.812185
C	-1.204176	4.016041	-0.383069
C	0.023071	4.251860	-1.029153
H	0.566245	3.405462	-1.453585
C	0.535703	5.545526	-1.141884
H	1.485570	5.710732	-1.659917
C	-0.161617	6.628064	-0.593145
H	0.241818	7.642140	-0.675880
C	-1.375401	6.405736	0.066022
H	-1.921052	7.244219	0.509805
C	-1.894873	5.112205	0.165696
H	-2.834422	4.954863	0.701165

S3. References

[1] K. Suzuki, A. Kobayashi, S. Kaneko, K. Takehira, T. Yoshihara, H. Ishida, Y. Shiina, S. Oishi, S. Tobita, *Phys. Chem. Chem. Phys.* **2009**, *11*, 9850–9860.

[2] *a*) N. Hellou, M. Srebro-Hooper, L. Favereau, F. Zinna, E. Caytan, L. Toupet, V. Dorcet, M. Jean, N. Vanthuyne, J. A. G. Williams, L. Di Bari, J. Autschbach, J. Crassous, *Angew. Chem. Int. Ed.* **2017**, *56*, 8236–8239; *b*) A. Macé, N. Hellou, J. Hammoud, C. Martin, E. S. Gauthier, L. Favereau, T. Roisnel, E. Caytan, G. Nasser, N. Vanthuyne, J. A. G. Williams, F. Berrée, B. Carboni, J. Crassous, *Helv. Chim. Acta*, **2019**, *102*, e1900044.

[3] E. S. Gauthier, L. Abella, N. Hellou, B. Darquié, E. Caytan, T. Roisnel, N. Vanthuyne, L. Favereau, M. Srebro-Hooper, J. A. G. Williams, J. Autschbach, J. Crassous, *Angew. Chem. Int. Ed*. **2020**, *59*, 8394–8400.

[4] Gaussian 16, Revision C.01, M. J. Frisch, G. W. Trucks, H. B. Schlegel, G. E. Scuseria, M. A. Robb, J. R. Cheeseman, G. Scalmani, V. Barone, G. A. Petersson, H. Nakatsuji, X. Li, M. Caricato, A. V. Marenich, J. Bloino, B. G. Janesko, R. Gomperts, B. Mennucci, H. P. Hratchian, J. V. Ortiz, A. F. Izmaylov, J. L. Sonnenberg, D. Williams-Young, F. Ding, F. Lipparini, F. Egidi, J. Goings, B. Peng, A. Petrone, T. Henderson, D. Ranasinghe, V. G. Zakrzewski, J. Gao, N. Rega, G. Zheng, W. Liang, M. Hada, M. Ehara, K. Toyota, R. Fukuda, J. Hasegawa, M. Ishida, T. Nakajima, Y. Honda, O. Kitao, H. Nakai, T. Vreven, K. Throssell, J. A. Montgomery, Jr., J. E. Peralta, F. Ogliaro, M. J. Bearpark, J. J. Heyd, E. N. Brothers, K. N. Kudin, V. N. Staroverov, T. A. Keith, R. Kobayashi, J. Normand, K. Raghavachari, A. P. Rendell, J. C. Burant, S. S. Iyengar, J. Tomasi, M. Cossi, J. M. Millam, M. Klene, C. Adamo, R. Cammi, J. W. Ochterski, R. L. Martin, K. Morokuma, O. Farkas, J. B. Foresman, and D. J. Fox, Gaussian, Inc., Wallingford CT, 2016.

[5] F. Weigend, R. Ahlrichs, *Phys. Chem. Chem. Phys.* **2005**, *7*, 3297–3305.

[6] J. M. L. Martin, A. Sundermann, *J. Chem. Phys.* **2001**, *114*, 3408–3420.

[7] D. Andrae, U. Häußermann, M. Dolg, H. Stoll, H. Preuß, *Theor. Chim. Acta* **1990**, *77*, 123–141.

[8] J. Tomasi, B. Mennucci, R. Cammi, *Chem. Rev.* **2005**, *105*, 2999–3094.

[9] M. Cossi, V. Barone, R. Cammi, J. Tomasi, *Chem. Phys. Lett.* **1996**, *255*, 327–335.

[10] V. Barone, M. Cossi, *J. Phys. Chem. A* **1998**, *102*, 1995–2001.

[11] M. Cossi, V. Barone, *J. Chem. Phys.* **2001**, *115*, 4708–4717.

[12] G. Scalmani, M. J. Frisch, *J. Chem. Phys.* **2010**, *132*, 114110.

[13] A. D. Becke, *J. Chem. Phys.* **1993**, *98*, 5648–5652.

[14] C. Lee, W. Yang, R. G. Parr, *Phys. Rev. B*, **1988**, *37*, 785–789.

[15] P. J. Stephens, F. J. Devlin, C. F. Chabalowski, M. J. Frisch, *J. Phys. Chem.* **1994**, *98*, 11623–11627.

[16] A. D. Becke, *J. Chem. Phys.* **1993**, *98*, 1372–1377.

[17] C. Adamo, V. Barone, *J. Chem. Phys.* **1999**, *110*, 6158–6169.

[18] M. Ernzerhof, G. E. Scuseria, *J. Chem. Phys.* **1999**, *110*, 5029–5036

[19] GaussView, Version 5.0.9, R. Dennington, T. A. Keith, J. M. Millam, Semichem Inc., Shawnee Mission, KS, 2009.

[20] T. Yanai, D. P. Tew, N. C. Handy, *Chem*. *Phys*. *Lett*. **2004**, *393*, 51–57.

[21] I. Tamm, *J. Phys. USSR* **1945**, *9*, 449–460.

[22] S. M. Dancoff, *Phys. Rev.* **1950**, *78*, 382–385.

[23] S. Hirata, M. Head-Gordon, *Chem. Phys. Lett.* **1999**, *314*, 291–299.

[24] M. J. G. Peach, M. J. Williamson, D. J. Tozer, *J. Chem. Theory Comput.* **2011**, *7*, 3578–3585.

[25] M. J. G. Peach, D. J. Tozer, *J. Phys. Chem. A* **2012**, *116*, 9783–9789.

[26] M. J. G. Peach, N. Warner, D. J. Tozer, *Mol. Phys.* **2013**, *111*, 1271–1274.

[27] C. Shen, E. Anger, M. Srebro, N. Vanthuyne, K. K. Deol, T. D. Jefferson, G. Muller, J. A. G. Williams, L. Toupet, C. Roussel, J. Autschbach, R. Reau, J. Crassous, *Chem. Sci.* **2014**, *5*, 1915–1927.

[28] E. Anger, M. Srebro, N. Vanthuyne, C. Roussel, L. Toupet, J. Autschbach, R. Reau, J. Crassous, *Chem. Commun.* **2014**, *50*, 2854–2856.

[29] N. Saleh, M. Srebro, T. Reynaldo, N. Vanthuyne, L. Toupet, V. Y. Chang, G. Muller, J. A. G. Williams, C. Roussel, J. Autschbach, J. Crassous, *Chem. Commun.* **2015**, *51*, 3754–3757.

[30] H. D. Ludowieg, M. Srebro-Hooper, J. Crassous, J. Autschbach, *Chemistry Open*, **2022**, *11*, e202200020.